NTT DOCOMO

Technical Journal

vol.19 No.1 | Jul.2017

DOCOMO Today

- Achieving Personal Agents and Pursuing Collaboration

Technology Reports

- Base-station Equipment and Router-type Mobile Terminal Supporting 4×4 MIMO and 256QAM for 682 Mbps Maximum on Downlink
- Latest Radio Access Technologies for 5G Systems and Field Testing Results - Technologies Realizing Ultra-high-speed Data Transport, High-speed Mobility, and Improved Spectral Efficiency -
- Expanding Viewing Angle in Head-mounted Displays Considering Field-of-view Characteristics

NTT docomo

Achieving Personal Agents and Pursuing Collaboration

General Manager of
Service Innovation Department
Tomoyoshi Ohno

In 2013, NTT DOCOMO announced its goal of becoming a Smart Life Partner to better serve its customers. Since then, we have undertaken the development of "personal agents" that seamlessly fit into people's lives as a key objective. A personal agent has a close relationship with the user providing 24/7 support to enrich that person's life in all sorts of scenarios. Rather than just an agent acting on behalf of a person, a personal agent helps the user in deciding what action to take in a particular situation.

There are three main elements to achieving personal agents: technology, big data, and engineers. In addition to establishing the requisite technology, it is also important that big data related to services be collected in some way and that engineers use that technology and data to develop actual personal agents.

As described in the talk "Personal Agents and Robot Initiatives" given at the 2015 DOCOMO R&D Open House, we have been developing three core technologies for achieving personal agents. These are natural language processing technology for achieving "ear and mouth" (aural and vocal) functions, image recognition technology for achieving an "eye" (visual) function, and user understanding/behavior-anticipation technology for achieving a "heart" (thoughtful) function. A "core technology" does not mean only in-house developed technology—it can also mean outside technologies that we can incorporate as needed and accumulated know-how as well. For this reason, we are proactively using open source products.

The basis of these core technologies is machine learning targeting big data, and in particular, deep learning*1, which is fast becoming the dominant form of machine learning. Deep learning is also included in these core technologies. By the way, Google's computer Go program AlphaGo™*2 incorporates deep learning, and it is famous for beating a professional Go player for the first time in 2015. In the case of games, playing rules and what constitutes winning or losing are clearly defined, so it is possible to adopt techniques for automatically learning winning methods by having two computers compete against each other. Given abundant computer power, it is relatively easy to uncover winning strategies. However, in the case of personal agents that we are developing, replies to user utterances proceed against the background of overall context, the personal relationship between the two speakers, etc., and there may not necessarily be only one correct reply. As a result, the application of deep learning is currently at the research stage and it is apparent that the development of practical personal agents is difficult. On the other hand, in the fields of speech recognition and image recognition in which labeled data are easy to obtain, the application of deep learning has entered the practical stage and has reached the point at which computers are coming to exceed the recognition abilities of human beings.

Since the appearance of deep learning, it has become possible to obtain superior results in an efficient manner by applying machine learning to large volumes of data compared with the conventional problem-solving approach using human knowledge and experiences. The issue here is how to go about acquiring such large volumes of data for learning purposes. We can look to natural language processing technology, the core technology of NTT DOCOMO's Shabette-Concier voice agent service launched in March 2012 (more than 36 million packages installed and more than 1.4 billion accesses as of the end of April 2016), for an answer. In the course of providing this service, this technology iteratively performs data collection, data analysis, and reflection of analysis results, thereby acquiring huge volumes of data with which machine learning can be performed in parallel. In this way, speech recognition performance and Q&A performance are being dramatically improved compared with conventional methods. In other words, to improve service performance and quality using deep learning, it is important to provide the service quickly and repeat the above cycle continuously to acquire a massive amount of data.

The widespread use of devices that can support this collection of big data is also important for achieving personal agents. Connecting the many things that surround us to the cloud will enable personal agents to learn about the wide variety of situations that people come to be in. We can envision the ultimate personal agent that can provide support for even the future behavior and health of the user.

From here on, we plan to actively pursue +d*3 (collaboration) that makes use of the core technologies needed for achieving personal agents. We have already partnered with TOMY in the joint development of OHaNAS®*4, an interactive conversational toy released in October 2015, using a natural-language dialog platform provided by NTT DOCOMO. The +d initiative can be thought of as the meeting of minds between two professional enterprises. OHaNAS is a typical example of this approach. Putting each other's strengths to work creates new value!

At present, we are promoting +d with taxi companies too. Our goal here is to predict the demand for taxis 30 minutes into the future by combining NTT DOCOMO demographic statistics with a taxi company's operational data plus other external data such as area characteristics and weather data and performing deep learning. I believe that predicting the future in this way is precisely an application of artificial intelligence using our core technologies that we have been refining continuously to achieve personal agents.

Going forward, we seek to create new value by leveraging the core technologies for achieving personal agents and collaborating with other companies on the mutual use of big data. In this way, we hope that the world I have described above will one day become commonplace. I look forward to the challenges that this endeavor brings.

*1 Deep learning: Machine learning using a neural network with a many-layer structure.
*2 AlphaGo™: A trademark or registered trademark of Google, Inc.
*3 +d: Name of NTT DOCOMO initiative for creating new value together with partner companies.
*4 OHaNAS®: A registered trademark of TOMY Company, Ltd.

NTT DOCOMO
Technical Journal
Vol.19 No.1 Jul. 2017

[Contents]

(P.4)

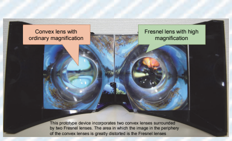

(P.30)

Topics 36

(P.36)

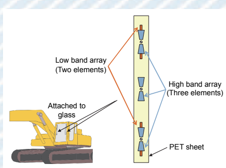

(P.41)

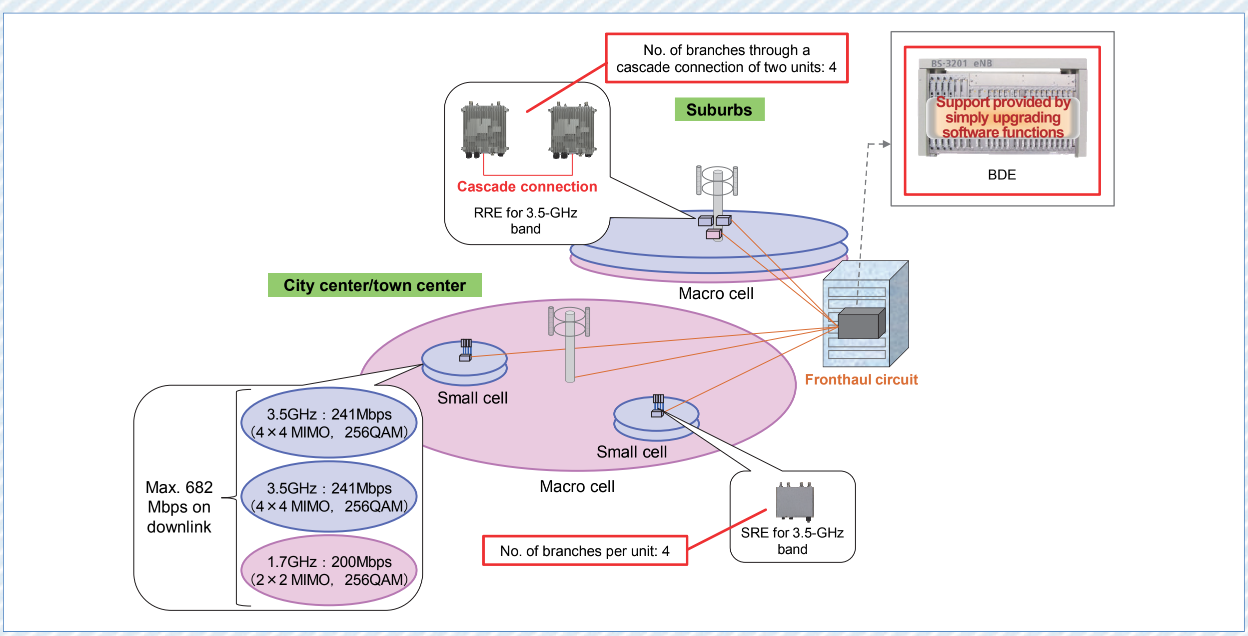

Technology Reports Base-station Equipment and Router-type Mobile Terminal Supporting 4×4 MIMO and 256QAM for Maximum Downlink Data Rate of 682 Mbps (P.4)

Network architecture supporting 4×4 MIMO and 256QAM

Technology Reports

4×4 MIMO | 256QAM | Advanced C-RAN

Base-station Equipment and Router-type Mobile Terminal Supporting 4×4 MIMO and 256QAM for 682 Mbps Maximum on Downlink

Radio Access Network Development Department Takafumi Shigefuji Rintaro Toba
Takahiro Takiguchi Takayuki Isogawa
Communication Device Development Department Takayuki Furuta

NTT DOCOMO launched mobile communication services called PREMIUM 4G with a maximum data rate of 225 Mbps on the downlink in March 2015. It then began services with a maximum downlink data rate of 375 Mbps by enhanced CA technology in May 2016 and services with a maximum downlink data rate of 370 Mbps using TDD in the 3.5-GHz band in June 2016. Since then, we have developed base-station equipment and a router-type mobile terminal supporting 4×4 MIMO technology and 256QAM technology to increase downlink data rate even further, and by combining these technologies with deployed CA technology, we launched commercial services with a maximum downlink data rate of 682 Mbps in March 2017. In this article, we describe 4×4 MIMO and 256QAM technologies and present base-station equipment and a router-type mobile terminal for achieving a maximum downlink data rate of 682 Mbps.

1. Introduction

The demand for higher data rate in the mobile network has been growing as the use-case of applications for smartphones and high-volume content services oriented to smartphones expands.

In March 2015, NTT DOCOMO launched mobile communication services with a maximum data rate of 225 Mbps on the downlink as PREMIUM 4G. Then, in May 2016, it began services with a maximum downlink data rate of 375 Mbps by enhanced Carrier Aggregation (CA)*1 technology, and

*1 CA: A technology that achieves high data rate communications through bandwidth expansion while maintaining backward compatibility with existing LTE by performing simultaneous transmission and reception using multiple component carriers.

in June of 2016, it began services with a maximum downlink data rate of 370 Mbps using Time Division Duplex (TDD)*2 in the 3.5-GHz band [1]. We have since developed base-station equipment and a router-type mobile terminal supporting 4×4 Multiple Input Multiple Output (MIMO)*3 technology and 256 Quadrature Amplitude Modulation (QAM)*4 technology to achieve a dramatic increase in maximum data rate. Then, in March 2017, we combined these technologies with deployed CA technology to launch commercial services with a maximum downlink data rate of 682 Mbps, which represents a threefold increase compared with the maximum data rate at the time of the PREMIUM 4G launch.

NTT DOCOMO successfully deployed PREMIUM 4G and increased the data rate efficiently through the application of Advanced Centralized Radio Access Network (Advanced C-RAN)*5 architecture [2]. Furthermore, by designing the base-station equipment to configure this Advanced C-RAN architecture with enough future extensions, we were able to provide new mobile communication services supporting 4×4 MIMO and 256QAM by simply adding functions to the software of existing base-station equipment. This made it possible to provide coverage areas supporting a maximum downlink data rate of 682 Mbps in an economical and early manner.

In this article, we describe these 4×4 MIMO and 256QAM technologies and present base-station equipment and a router-type mobile terminal that can support a maximum downlink data rate of 682 Mbps.

2. Data Rate-enhancing Technologies

2.1 4×4 MIMO

Applying more advanced MIMO technology can improve the maximum downlink data rate. At NTT DOCOMO, we have developed 4×4 MIMO technology using four antennas as an advancement to 2×2 MIMO with two antennas, which we have been using up to now. The following describes this technology in detail.

1) Four-stream Transmission

(1) Overview

In MIMO transmission, the number of simultaneous transmission data sequences to be multiplexed is called the "number of streams." In 2×2 MIMO, a maximum of two streams can be transmitted, but in 4×4 MIMO, the ability to transmit a maximum of four streams at once enables approximately twice the amount of transmission data thereby increasing the maximum data rate. In LTE specifications, there are multiple Transmission Mode (TM) specifications for achieving 4×4 MIMO. For example, TM3 and TM4 specified in the LTE Release 8 specification (hereinafter referred to as "LTE Rel. 8") support the transmission by a maximum of four streams using four antennas worth of a Cell-specific Reference Signal (Cell-specific RS)*6. In addition, TM9 and TM10 specified in LTE Rel. 10 and LTE Rel. 11, respectively, support flexible precoding and Multi-User MIMO*7. In those TMs, Channel State Information-Reference Signal (CSI-RS)*8 and User Equipment-specific RS (UE-specific RS)*9 are specified

*2 TDD: A bidirectional transmit/receive system. It achieves bidirectional communication by allocating different time slots to uplink and downlink transmissions that use the same frequency band.

*3 MIMO: A technology for achieving high data rate transmission by simultaneously transmitting different signals from multiple antennas.

*4 QAM: A modulation method using both amplitude and phase.

*5 Advanced C-RAN: Network architecture promoted by NTT DOCOMO using CA technology to achieve inter-cell coordination between macro cells and small cells.

*6 Cell-specific RS: A reference signal specific to each cell for measuring received quality in the downlink.

*7 Multi-User MIMO: Technology that uses MIMO transmission over the same time and frequency for multiple users.

in addition to Cell-specific RS to perform four-stream transmission [3]. That is, in TM3/4, only Cell-specific RS is used for measurement of the channel connectivity quality and channel state information for transmission data and for demodulation of transmission data on the downlink. In TM9/10, meanwhile, Cell-specific RS is used for measurement of the channel connectivity quality, CSI-RS for measurement of channel state information for transmission data, and UE-specific RS for demodulation of transmission data (**Figure 1**).

(2) 3GPP standardization approach

The original specifications had two key issues for TM9/10. NTT DOCOMO studied and proposed ways of improving these specifications thereby contributing to higher data rates.

- The first issue is a limitation on data transmission resources in the transmission timing of the synchronization signal. The frequency resource, the Resource Block (RB), allocated for transmission of the synchronization signal cannot be used for transmission of UE-specific RSs, so the TM9/10 transmission data cannot be allocated to those RBs. Moreover, a base station cannot allocate in units of RBs but in units of RB groups within some of the RBs for transmission to a mobile terminal. In the original specifications for TM9/10, transmission data could be allocated neither within the individual RBs used for transmitting the synchronization signal nor throughout the RB groups that include those RBs, which unnecessarily limited data transmission resources. In response to this issue, the specifications were revised to enable the RBs located within the RB groups containing the synchronization signal but not actually transmitting the synchronization signal to be used for data transmission (**Figure 2**).

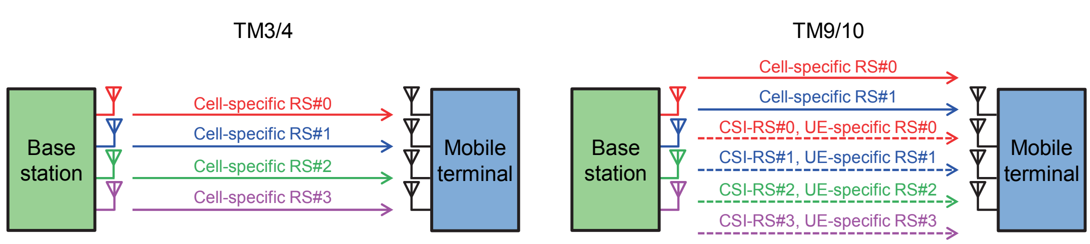

Application	TM3/4	TM9/10
Measurement of channel connectivity quality	Cell-specific RS	Cell-specific RS
Measurement of channel state information for transmission data	Cell-specific RS	CSI-RS
Demodulation of transmission data	Cell-specific RS	UE-specific RS

Figure 1　RSs used for various TMs

*8　CSI-RS: A reference signal transmitted from each antenna to measure the state of the radio channel.

*9　UE-specific RS: A reference signal specifically for UE for demodulating the data signal in the downlink.

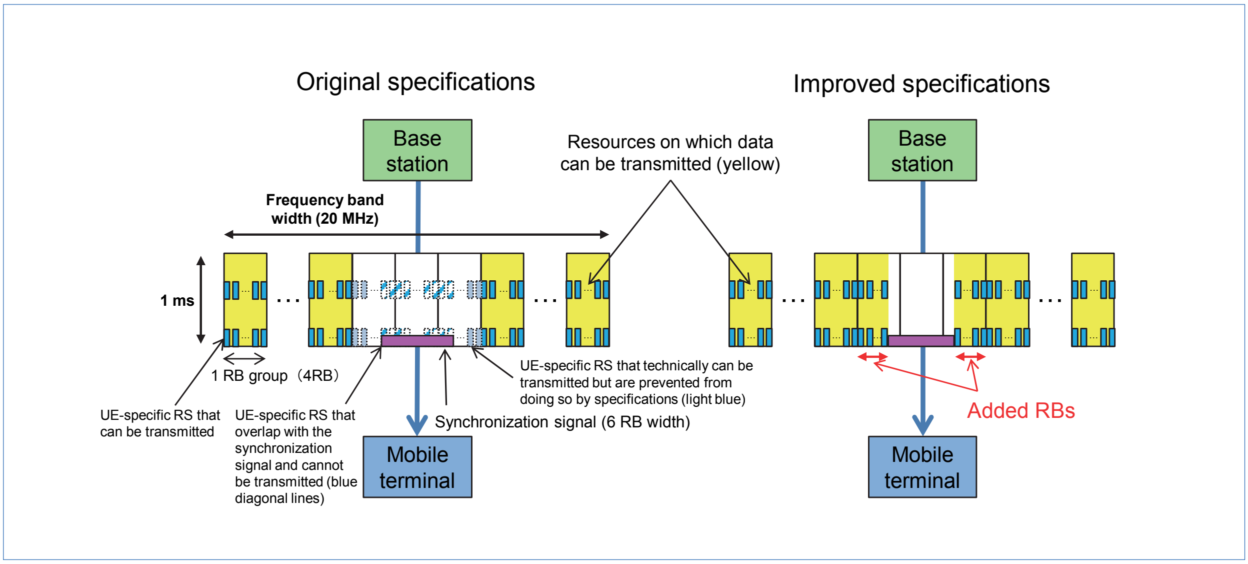

Figure 2　Easing of resource limit in transmission timing of synchronization signal

- The second issue is that the addition of RS overhead*10 in TM9/10 prevents the maximum amount of data in the original specifications from being transmitted. Several transmission bit patterns for the transmission time interval are established in the specifications. In the case of TM9/10, however, the amount of data achieving the maximum data rate cannot be allocated due to the RS overhead, so the maximum amount of transmission data is limited requiring the base station to allocate the data without the maximum data rate pattern. Consequently, as the amount of transmission data at one time was limited in this way, the maximum data rate in TM9/10 could not be achieved in base-station equipment and mobile terminals. For this issue, we defined a new data-usage pattern taking RS overhead into account for TM9/10 specifications. As a result, we achieved a higher maximum data rate in base-station equipment and mobile terminals performing communications by TM9/10 (**Figure 3**).

2) Beamforming Based on Feedback

Base-station equipment forms optimal beams by using feedback information from a mobile terminal. This beamforming process improves not only the maximum data rate but channel quality as well. On the transmission side, the base station controls the amplitudes and phases on multiple antennas to form a directional pattern to increase or decrease antenna gain in specific directions. A base station can form the beams more powerfully by using four transmission antennas on 4×4 MIMO compared with 2×2 MIMO transmission. The mobile terminal, meanwhile, estimates the propagation channel using received RSs and reports an appropriate optimal beam pattern to

*10 Overhead: Control information needed for transmitting/receiving user data, plus radio resources used for other than transmitting user data such as reference signals for measuring received quality.

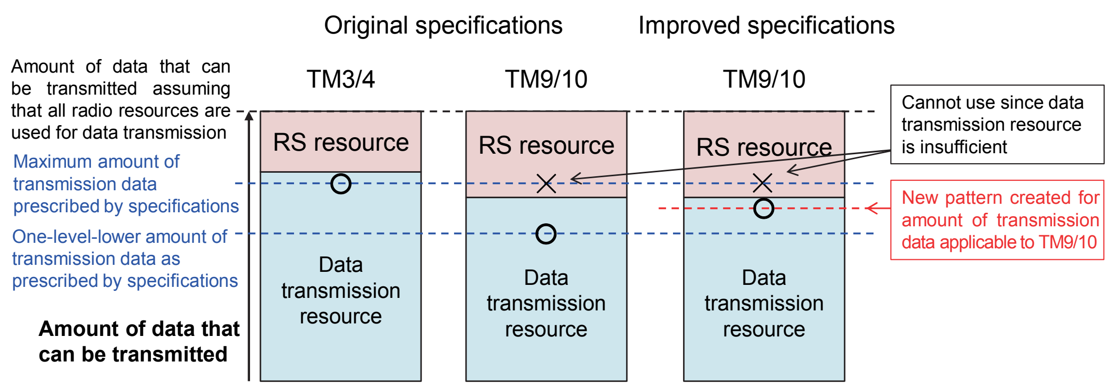

Figure 3　New pattern for amount of transmission data considering RS overhead

base-station equipment as a Precoding Matrix Indicator (PMI)*11. As feedback information, this PMI is returned together with the Channel Quality Indicator (CQI)*12 and Rank Indicator (RI)*13, the latter of which indicates the optimal number of streams. The base-station equipment now references the PMI and determines precoding weights*14 for the transmission signal sent to the mobile terminal. Finally, for TM3/4, the mobile terminal demodulates the data signal by referencing precoding information received from the base-station equipment, and for TM9/10, by referencing the UE-specific RS using the same precoding as transmission data.

3) Determining an Optimal Combination of Streams and Beamforming

There is a trade-off between number of streams and the beamforming effect: simply put, transmission with multiple streams reduces the beamforming effect. For this reason, the base-station equipment uses the feedback information reported by the mobile terminal, the amount of transmission data, etc. to decide on the optimal number of streams and the precoding to be used in beamforming. Finding an appropriate combination of number of streams and beamforming makes it possible to improve maximum data rate through multiple streams in areas with high quality near the base station and to improve received quality by beamforming in areas with low quality such as the cell edge (**Figure 4**).

2.2 256QAM

Higher data rates can be achieved by adopting a method that can transmit multiple bits per symbol*15 (multi-value modulation*16). NTT DOCOMO decided to support 256QAM for this reason. As a higher modulation scheme specified by LTE Rel. 12, 256QAM can transmit a maximum of 8 bits per symbol, which means that a downlink data rate approximately 1.3 times faster than that of 64QAM can be expected (**Figure 5**).

The use of a higher modulation scheme like

*11 PMI: Information fed back from the mobile terminal on precoding assumed to be optimal for the downlink.

*12 CQI: Information fed back from the mobile terminal on downlink quality.

*13 RI: Information fed back from the mobile terminal on the number of streams assumed to be optimal on the downlink.

*14 Precoding weights: Phase differences applied to each transmitting antenna during beamforming.

*15 Symbol: A unit of data for transmission. In Orthogonal Frequency Division Multiplexing (OFDM), it comprises multiple subcarriers. Multiple bits (2 bits in the case of Quadrature Phase Shift Keying (QPSK)) map to each subcarrier.

*16 Multi-value modulation: A modulation system that includes two or more bits of information in one signal.

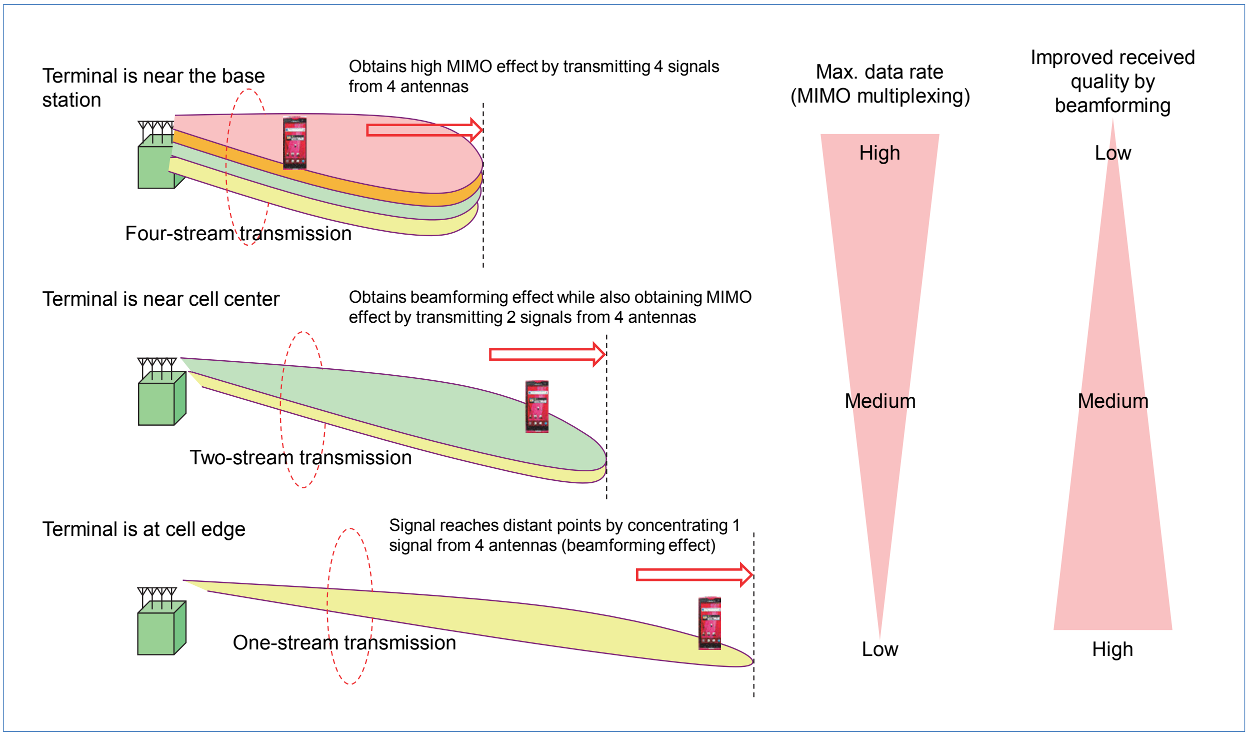

Figure 4 Number of streams and beamforming effect

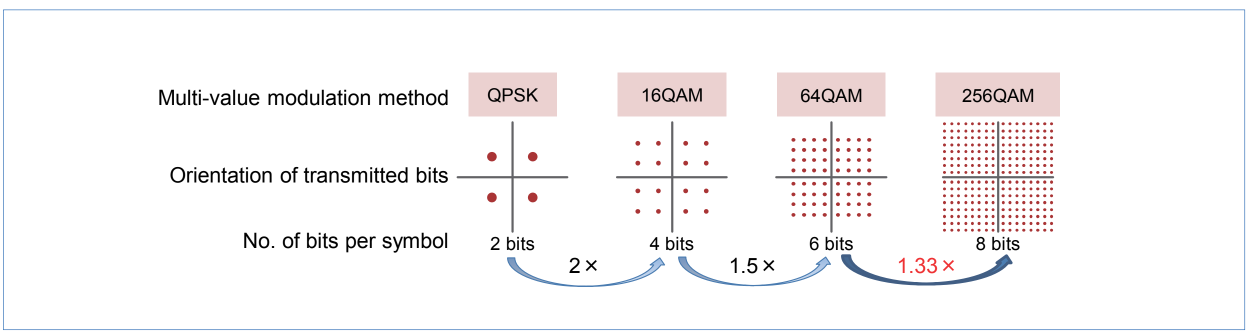

Figure 5 256QAM

256QAM requires a high-quality wireless environment, that is, an environment with a high Signal-to-Interference plus Noise power Ratio (SINR)*17. As a consequence, not all mobile terminals can necessarily use 256QAM all the time, and for this reason, the base-station equipment decides what modulation scheme a mobile terminal will use based on the CQI index reported by that terminal. The maximum data rate can be improved using 256QAM for a mobile terminal reporting a high CQI index.

To avoid having to increase the number of CQI indices on introducing 256QAM in LTE Rel. 12, the specification for the existing CQI table was modified so as to replace some of the indices with

*17 SINR: Ratio of desired received signal power to that of other received signals (interfering signals from other cells or sectors and thermal noise).

CQI indices corresponding to 256QAM [4] (**Figure 6**). Both the base-station equipment and mobile terminal store the existing 256QAM-non-supported CQI table and the 256QAM-supported CQI table, and the base-station equipment informs the mobile terminal which table to use taking into account its current capability.

3. Base-station Equipment Supporting 4×4 MIMO and 256QAM

As described in section 2.1, the number of antennas must be increased from two to four to support 4×4 MIMO. NTT DOCOMO decided to introduce 4×4 MIMO in the 3.5-GHz band for two main reasons: the high frequencies of this band enable antenna downsizing and the availability of a 40 MHz bandwidth in this band makes for a high data rate-enhancing effect.

The network architecture supporting 4×4 MIMO and 256QAM is shown in **Figure 7**. This architecture can achieve a maximum data rate of 682 Mbps on the downlink by applying both 4×4 MIMO and 256QAM to the 3.5 GHz band and only 256QAM to the other frequency bands. This is made possible by a CA configuration that combines the 3.5-GHz band having a 40 MHz bandwidth using TDD with the other frequency bands having a maximum 20 MHz bandwidth using Frequency Division Duplex (FDD)*18. The low power Small optical remote Radio Equipment (SRE)*19 that configures small cells in the 3.5-GHz band was originally developed as a unit consisting of four transceiver systems (branches) with consideration to supporting 4×4 MIMO, so SREs that had already been deployed could be immediately used as 4-branch

256QAM non-supported

CQI index	Modulation method	Code rate
0	out of range	
1	QPSK	0.076
2	QPSK	0.117
3	QPSK	0.188
4	QPSK	0.301
5	QPSK	0.438
6	QPSK	0.588
7	16QAM	0.369
8	16QAM	0.479
9	16QAM	0.602
10	64QAM	0.455
11	64QAM	0.554
12	64QAM	0.650
13	64QAM	0.754
14	64QAM	0.853
15	64QAM	0.926

QPSK area reduced

Shift upward by filling in the gap

256QAM supported

CQI index	Modulation method	Code rate
0	out of range	
1	QPSK	0.076
2	QPSK	0.188
3	QPSK	0.438
4	16QAM	0.369
5	16QAM	0.479
6	16QAM	0.602
7	64QAM	0.455
8	64QAM	0.554
9	64QAM	0.650
10	64QAM	0.754
11	64QAM	0.853
12	256QAM	0.694
13	256QAM	0.778
14	256QAM	0.864
15	256QAM	0.926

256QAM added by shifting existing CQI upward

Figure 6 256QAM non-supported/supported CQI tables

*18 FDD: A scheme for transmitting signals using different carrier frequencies and bands on the uplink and downlink.

*19 SRE: Radio equipment for small cells installed in places remotely located from BDE (see *21) using optical fiber, etc.

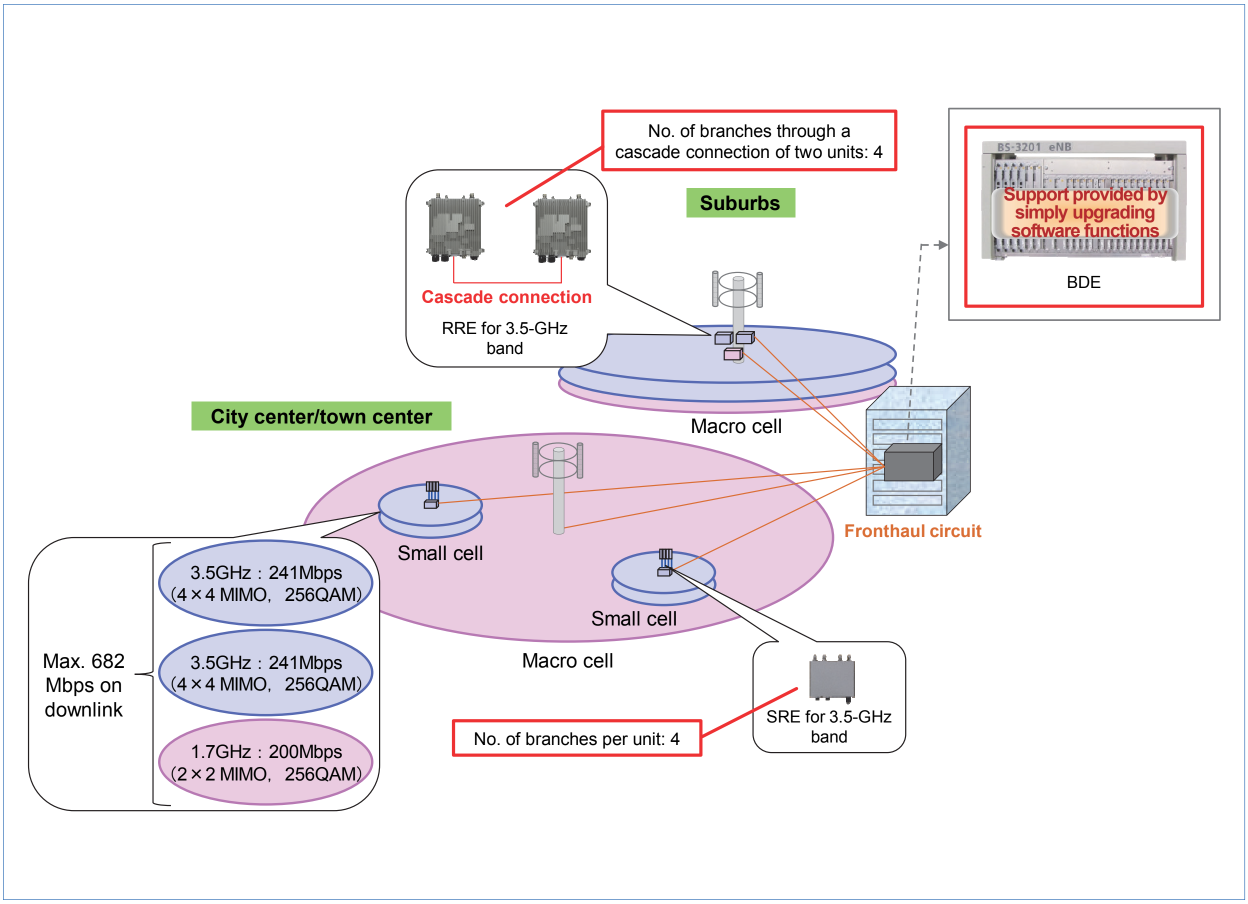

Figure 7 Network architecture supporting 4×4 MIMO and 256QAM

base-station equipment. In addition, the Remote Radio Equipment (RRE)*20 for macro cells in the 3.5-GHz band, while consisting of two branches per unit taking into account equipment size at the time of 2×2 MIMO deployment, have been designed to operate as 4-branch base-station equipment through a cascade connection of two units. As a result, 4×4 MIMO can be supported in a macro cell by adding and connecting in cascade one RRE unit to a previously deployed RRE unit. In both small cells and macro cells, 4×4 MIMO can be achieved by simply adding functions to the software of the Base station Digital processing Equipment (BDE)*21 and SRE/RRE units.

Furthermore, base-station equipment supporting 4×4 MIMO can transmit 2×2 MIMO signals with its four antennas to an existing UE supporting 2×2 MIMO thereby increasing total transmission power of the base station and raising the received level at the UE.

At the same time, adding 256QAM functions to BDE software makes it possible to support 256QAM in all areas of existing base-station equipment regardless of FDD or TDD use.

*20 RRE: Radio equipment installed in places remotely located from BDE (see *21) using optical fiber, etc.

*21 BDE: Digital signal processing equipment for base stations in the LTE system, equipped with a baseband processing section and maintenance/monitoring functions.

4. Router-type Mobile Terminal Supporting 4×4 MIMO and 256QAM

4.1 Overview

The external appearance of a newly developed router-type mobile terminal is shown in **Photo 1**. This mobile terminal operates by 4×4 MIMO in the 3.5-GHz TDD band and supports 256QAM. As in the case of base-station equipment, it achieves a maximum data rate of 682 Mbps on the downlink by applying 4×4 MIMO and 256QAM simultaneously in a CA configuration that combines the 3.5-GHz band having a 40 MHz bandwidth with other frequency bands having a FDD 20 MHz bandwidth.

Photo 1 External appearance of router-type mobile terminal supporting 4×4 MIMO

4.2 Antenna Configuration

The antenna arrangement in this router-type mobile terminal supporting 4×4 MIMO is shown in **Figure 8**. Among these four antennas, one operates as a main antenna having both transmitting and receiving functions while the other three operate as sub-antennas having only a receiving function. In addition to the 3.5-GHz band, both the main antenna and sub-antennas support other cellular frequency bands (2 GHz, 1.7 GHz, etc.).

Metallic components such as Wi-Fi®*22 antennas, battery, display, and substrates mounting various

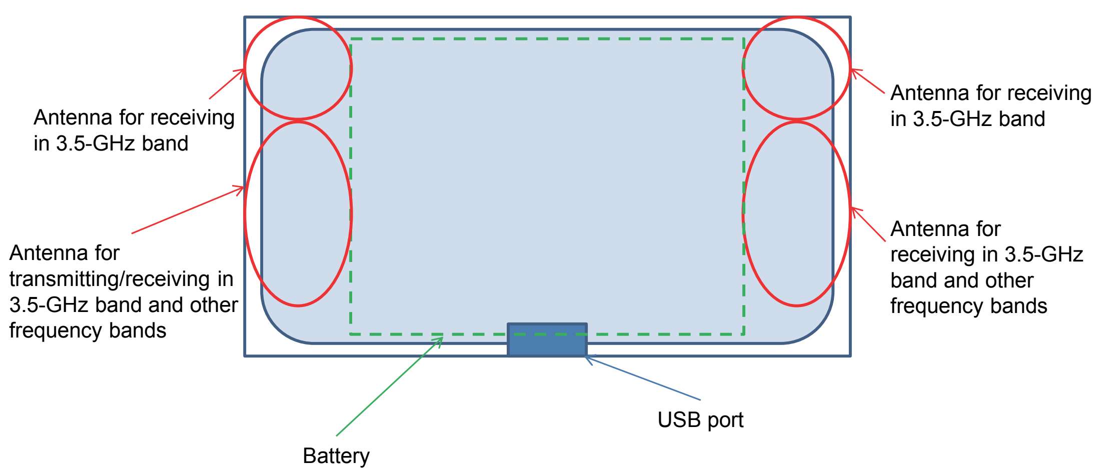

Figure 8 Antenna arrangement in router-type mobile terminal supporting 4×4 MIMO

*22 Wi-Fi®: A registered trademark of the Wi-Fi Alliance.

devices in the vicinity of a cellular antenna can affect antenna performance. Consequently, to maintain antenna performance while preserving the compact configuration (62×98×13.6 mm) of this mobile terminal, the antennas must be kept a certain distance from other metallic components.

On the other hand, there is concern that arranging two 3.5-GHz band antennas in close proximity to each other will result in high inter-antenna correlation*23, which can prevent MIMO performance from being sufficiently demonstrated and degrade the data rate. In response to this concern, we devised a measure for keeping antenna correlation low even for antennas in a close-proximity arrangement in combination with existing technology for downsizing antennas accommodating multiple frequencies.

In this mobile terminal, we also adopted the USB 3.0 standard to meet the need for increasing the data rate of the unit's external interface to keep up with increases in radio data rates. However, the use of such a USB interface with a high data rate can increase the amount of noise added to the cellular frequency bands and negatively affect downlink performance. We therefore incorporated several noise countermeasures to prevent this degradation in performance such as enhancing the metallic shield around the USB connector, adding a noise-removal filter, and optimizing the connector and antenna position. These measures help prevent a drop in data rate at the time of USB tethering*24.

4.3 Evaluation of Antenna Performance

The 4×4 MIMO antenna measurement system for the developed router-type mobile terminal is shown in **Figure 9**. The configuration shown here is for a 3 DownLink CA (3DL CA) consisting of a FDD frequency band + 3.5-GHz + 3.5-GHz (where the 3.5-GHz band is used for 4×4 MIMO). We used this measurement system to evaluate downlink data rate from base-station equipment to the mobile terminal. In the figure, a reverberation chamber is used to construct a fading*25 environment in which signals from the base-station equipment arrive at the Device Under Test (DUT) from various directions.

An LTE signal is generated for each Component Carrier (CC)*26, so in this measurement system, 4×4 MIMO signals consisting of signal 1 of Secondary CC (SCC)*27 1 (SCC1 p1) and signal 1 of SCC 2 (SCC2 p1) are combined by a combiner unit and transmitted from a single antenna. The same configuration holds for signals SCCp2 – p4, but Primary CC (PCC)*28 signals are transmitted from separate antennas. This system simulates CA on the downlink consisting of FDD 2×2 MIMO + 3.5-GHz 4×4 MIMO + 3.5-GHz 4×4 MIMO signals.

We evaluated the downlink data rate for the DUT using this measurement system and confirmed that a maximum performance of 682 Mbps could be guaranteed for a 4×4 MIMO, 256QAM, 3DL CA configuration.

5. Conclusion

In this article, we introduced 4×4 MIMO and 256QAM technologies to increase the maximum data rate in the downlink of NTT DOCOMO PREMIUM 4G. We also described base-station equipment and

*23 Correlation: An index expressing similarity between different signals. Expressed as a complex number, its absolute value ranges from 0 to 1. Similarity increases as the value approaches 1, in which case signal separation at the receiver is difficult resulting in degraded throughput in MIMO communications.

*24 Tethering: A function which enables a mobile terminal to be used as an external modem, so that Wi-Fi devices such as game machines or PCs can connect to the Internet through the mobile phone's connection.

*25 Fading: A phenomenon in mobile communications in which radio signals having different propagation paths due to reflection, etc. arrive at different times thereby affecting amplitude and phase.

*26 CC: In LTE, a carrier is treated as a single frequency block having a bandwidth of 20 MHz in both the uplink and downlink.

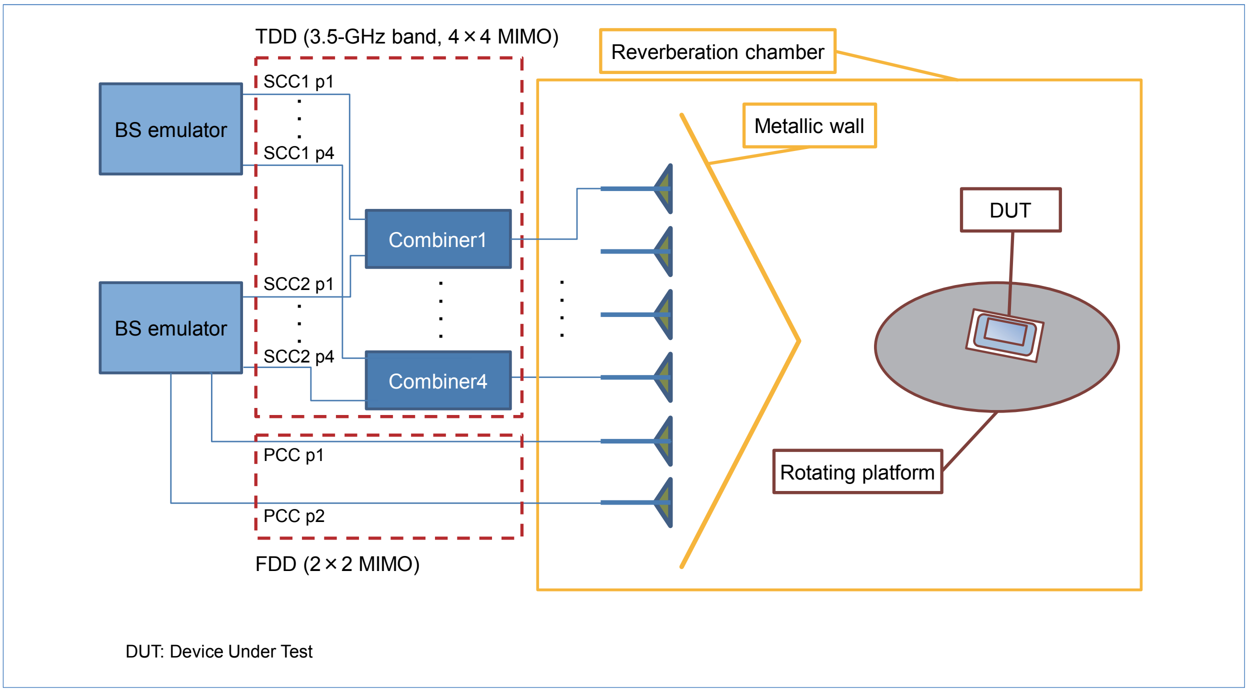

Figure 9 4×4 MIMO + 3DL CA throughput measurement system

a router-type mobile terminal for achieving a downlink data rate of 682 Mbps. Going forward, we plan to continue our development efforts toward even higher maximum data rates in PREMIUM 4G.

REFERENCES

[1] M. Fujii et al.: "Base-station Equipment with the Aim of Introducing 3.5-GHz band TD-LTE," NTT DOCOMO Technical Journal, Vol.18, No.2, pp.8–13, Oct. 2016.

[2] T. Yoshihara et al.: "Radio Equipment and Antennas for Advanced C-RAN Architecture," NTT DOCOMO Technical Journal, Vol.17, No.2, pp.19–24, Oct. 2015.

[3] 3GPP TS36.211 V12.8.0: "Evolved Universal Terrestrial Radio Access (E-UTRA); Physical channels and modulation (Release 12)," Dec. 2015.

[4] 3GPP TS36.213 V12.11.0: "Evolved Universal Terrestrial Radio Access (E-UTRA); Physical layer procedures (Release 12)," Sep. 2016.

*27 SCC: In CA, a carrier that provides radio resources in addition to PCC (see *28).

*28 PCC: In CA, a carrier that ensures connectivity between UE and the network.

Technology Reports Ultra-high-speed Data Communications High-speed Mobility Improved Spectral Efficiency

Latest Radio Access Technologies for 5G Systems and Field Testing Results

—Technologies Realizing Ultra-high-speed Data Transport, High-speed Mobility, and Improved Spectral Efficiency—

5G Laboratory, Research Laboratories Yoshihisa Kishiyama Satoshi Suyama Yukihiko Okumura

Various radio access technologies have been studied for 5G, to support wide frequency bands and a wide range of use cases. NTT DOCOMO has been collaborating with major global vendors to test these technologies. This article introduces some of the latest field testing results conducted with these vendors, including the first 20 Gbps high-speed data transmission tests done in collaboration with Ericsson, high-speed mobile data transmission tests done at 150 km/h on a racing circuit (the fastest in the world as of November 2016) done in collaboration with Samsung Electronics, and tests achieving very high spectral efficiency of up to 79.82 bps/Hz/cell done in collaboration with Huawei Technologies.

1. Introduction

Hopes are now raising around the world for the introduction of Fifth Generation mobile communications systems (5G) by the year 2020. Discussion at the 3GPP has begun on standards for a new 5G radio interface standard called New Radio (NR), and major organizations studying 5G in various countries are announcing plans for commercialization and testing of 5G [1]. NTT DOCOMO began studying 5G in 2010 and has promoted various activities such as proposing technology concepts, transmission testing, and leading discussion on standardization [2]. In particular, NTT DOCOMO has conducted testing of various 5G radio transmission technologies in collaboration with major global vendors, focused on high frequency-band, multi-antenna transmission technologies [3] that are being studied for 5G. Details of these were introduced in this journal [4]. This article describes highlights of the latest test results as of March 2017, from on-going 5G transmission testing being done in collaboration with major global vendors.

2. Testing Ultra-high-speed Communication

Use of high frequencies over 6 GHz for 5G, is being studied so that wide, continuous frequency bands of almost 1 GHz can be used. Massive Multiple Input Multiple Output (MIMO)*1 technology [3] with large numbers of antenna elements is used for such ultra-wideband transmission, applying techniques such as beam forming*2 and spatial multiplexing. This will enable mobile communication systems providing coverage with ultra-high-speed data communication of over 10 Gbps per user. NTT DOCOMO has been testing this sort of ultra-high-speed data communication using Massive MIMO in collaboration with Ericsson. Specifically, we have achieved communication speeds exceeding 10 Gbps with 800 MHz ultra-wideband transmission in the 15 GHz band, using MIMO transmission with up to four streams*3 per user and 256 Quadrature Amplitude Modulation (256QAM)*4. We have also achieved transmission exceeding 20 Gbps per base station [5] to multiple users simultaneously (total transmission speed to two users) with Multi-User MIMO (MU-MIMO)*5 and beam forming for the first time in an outdoor environment.

Results of joint ultra-high-speed data communication testing done with Ericsson are described below. These include an overview of the testing and results for ultra-high-speed MU-MIMO transmission achieving over 20 Gbps communication [6] as mentioned above, and for technical elements for Massive MIMO using multiple transmission points and reflections from buildings to increase communication speed [7] [8].

2.1 Testing Ultra-high-speed MU-MIMO Transmission

1) MU-MIMO Transmission Function and Equipment Overview

A schematic diagram of the MU-MIMO transmission function used in our tests is shown in **Figure 1**. The Base Station (BS) periodically sends a Mobility Reference Signal (MRS) (Fig. 1 (1)) for each candidate beam from the antenna units (called Radio Units (RU))*6, for use in beam selection. Mobile Stations (MS) use the MRS to calculate the MRS Received Power (MRSRP) for each beam. MSs compare the MRSRP of each beam and feedback the MRSRPs and beam ranking to the BS (Fig. 1 (2)). The BaseBand Unit (BBU)*7 in the BS selects the beam with the highest MRSRP for each MS (Fig. 1 (3)), transmitting beams from RU #1 and #2 to MS #1, and from RU #3 and #4 to MS #2 (Fig. 1 (4)).

External views of the RU are shown in **Figure 2**. Each RU consists of two antenna panels corresponding to horizontally and vertically polarized signals, enabling it to transmit two streams. Each antenna panel consists of a flat array antenna with 64 antenna elements at intervals of 0.7 λ. The antenna gain*8 is 24 deciBel isotropic (dBi)*9, and the transmission power per panel is 14 deciBel milli (dBm)*10. In our experiments, we used four RUs, transmitting up to eight streams to two users (for a theoretical peak transmission capacity of 31.2 Gbps).

2) Test Environment and Measurement Results

The tests were conducted in a 100 × 100 m

*1 **Massive MIMO:** Large-scale MIMO using a very large number of antenna elements. Since antenna elements can be miniaturized in the case of high frequency bands, Massive MIMO is expected to be useful in 5G.

*2 **Beam forming:** A technique for increasing or decreasing the gain of antennas in a specific direction by controlling the phase of multiple antennas to form a directional pattern of the antennas.

*3 **Stream:** A data sequence that is spatially-multiplexed when using multiple transceiver antennas with MIMO technology.

*4 **256QAM:** Quadrature Amplitude Modulation (QAM) is a modulation method using both amplitude and phase. In 256QAM, 256 (2^8) symbols exist, so this method allows for the transmission of 8 bits at one time.

*5 **MU-MIMO:** A technology that uses MIMO to transmit signals to multiple users at the same time using the same frequency.

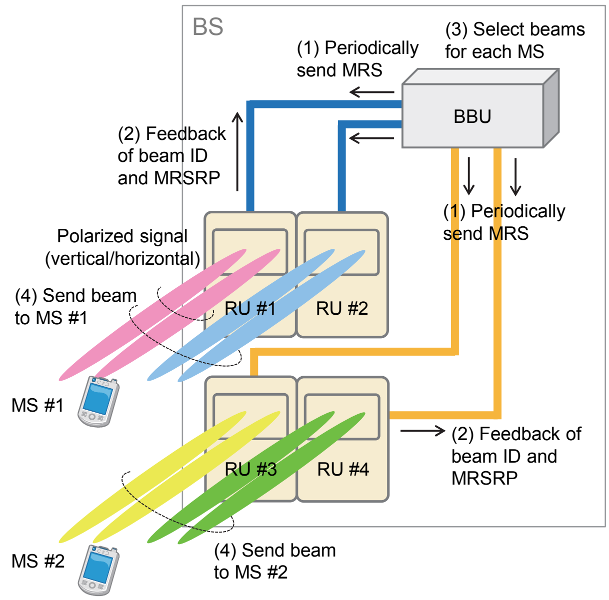

Figure 1　Test equipment MU-MIMO beam transmission function

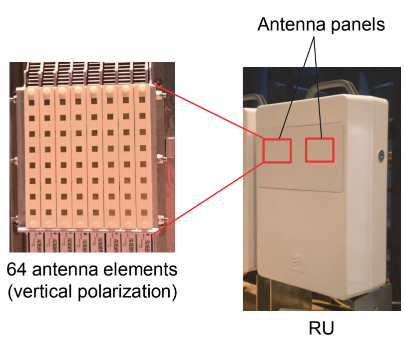

Figure 2　RU external views

area in the outdoor parking lot of the DOCOMO R&D Center in the YRP region of Yokosuka City, Kanagawa Prefecture. The measurement area was an open environment, providing Line-Of-Site (LOS)*11 conditions everywhere. MS #1 moved at walking speed (approx. 3 km/h) within the measurement area, while MS #2 was placed at fixed positions along the course.

The total transmission capacity (system throughput) characteristics for MU-MIMO transmission to two MSs, distributed according to MS #1 position and plotted in color on a map of the measurement area, is shown in **Figure 3**. In Fig. 3 (a), MS #2 is located near the edge of the measurement area, and in Fig. 3 (b) it is near the center.

The figures show that when the angular direction from the BS to MS #2 is different than the direction to MS #1, relatively higher system throughput is achieved. In particular, MS #2 is at the edge of the measurement area in Fig. 3 (a) (lower left), so when MS #1 is at the opposite side (upper right) of the measurement area, relatively high

*6 RU: Part of the equipment comprising a base station, which performs transmission and reception by converting digital signals to a radio signals, amplifying them and sending or receiving them from the antenna elements. It also performs processing necessary to generate beam forming for Massive MIMO.

*7 BBU: One component of base station equipment performing digital signal processing of transmit/receive information when communicating with a mobile terminal.

*8 Antenna gain: Radiated power in the direction of maximum radiation usually expressed as the ratio of radiated power to that of an isotropic antenna.

*9 dBi: A unit that describes antenna gain using a hypothetical isotropic antenna as the standard.

*10 dBm: Power value [mW] expressed as 10log (P). The value relative to a 1 mW standard (1 mW=0 dBm).

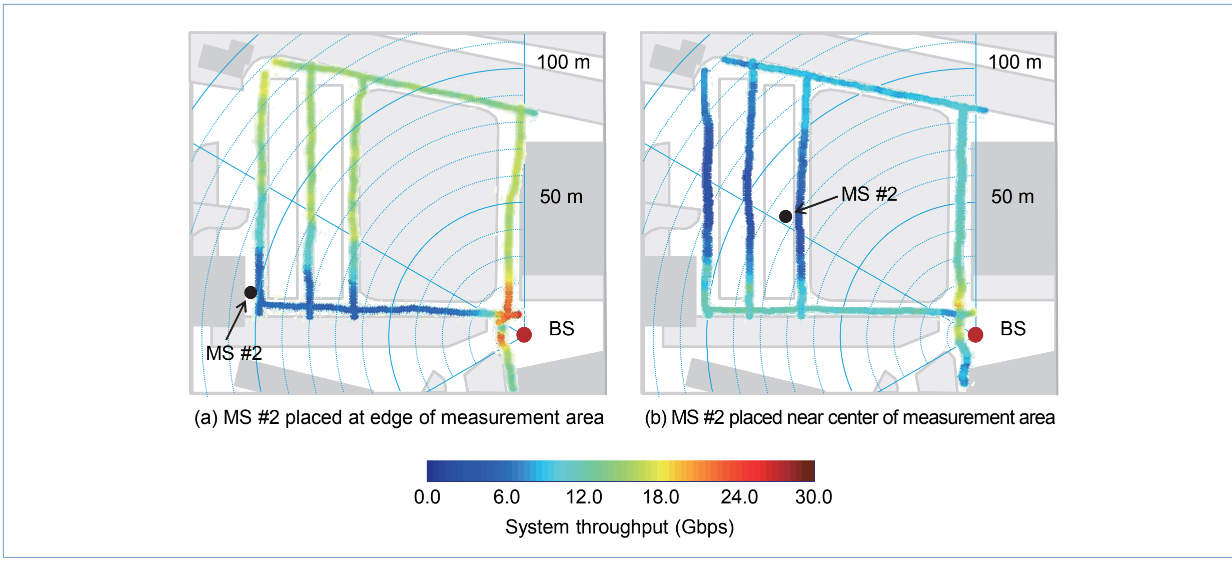

Figure 3 Ultra-high-speed MU-MIMO transmission test results

throughput between 15 and 20 Gbps is achieved. This is because when the angular directions to MS #1 and #2 are close, there is interference between the beams sent to each. High system throughput exceeding 20 Gbps is observed when the angular directions to each MS are farther apart and when MS #1 is relatively near to the BS. Specifically, system throughput of 25.9 Gbps was achieved when MS #1 was within 15 m of the BS in Fig. 3 (a), and 20.5 Gbps was achieved when MS #1 was within approximately 20 m of the BS in Fig. 3 (b).

2.2 Testing Elemental Technologies for Massive MIMO

Increasing propagation losses*12 and channel correlation*13 are two known issues due to the propagation characteristics of high frequency bands [4]. To resolve these issues, we have studied and tested technologies to improve communication speed, including beam forming with Massive MIMO to compensate for propagation losses as mentioned above, and use of multiple transmission points and reflections from buildings to reduce channel correlation.

1) Distributed MIMO Technology

Results from testing distributed MIMO*14 technology, which uses MIMO multiplexing to transmit separate streams from multiple transmission points, are shown in **Figure 4** [7]. Two RUs are used in these tests, transmitting the same beam for non-distributed MIMO, and different beams from RUs in different locations for distributed MIMO. The measurement course was the same as in Fig. 3, in the outdoor parking lot of the DOCOMO R&D Center. Throughput characteristics for non-distributed MIMO (two RUs at the same position) are shown in Fig. 4 (a), and for distributed MIMO (RUs placed 7 m apart) in Fig. 4 (b). Comparing these shows that applying distributed MIMO improved throughput characteristics greatly over the entire

*11 LOS: Describes an environment where there are no obstacles between the transmitter and receiver, allowing them to communicate via direct waves.

*12 Propagation losses: The amount of attenuation in the power of the signal emitted from the transmitting station till it arrives at the reception point.

*13 Channel correlation: An index indicating the similarity among multiple signals, with values near 1 (one) indicating similarity (correlation) and values near 0 (zero) indicating dissimilarity.

*14 Distributed MIMO: A MIMO transmission technology that transmits different MIMO streams from multiple base stations to a single mobile station.

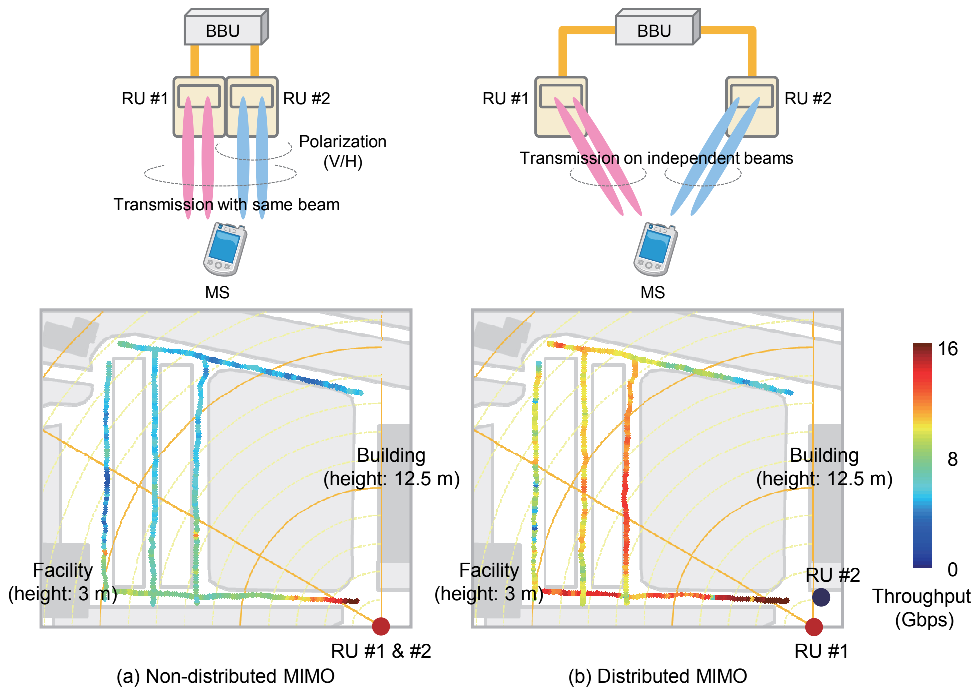

Figure 4 Test results of distributed MIMO technology

measurement area. This shows that transmitting different beams from different locations reduced channel correlation. When we checked the number of MIMO multiplexed streams (the rank), we found that the value for the cumulative distribution of 50% rose from 2.7 to 3.8, meaning that almost all of four streams (the maximum) were transmitted. As a result, we achieved throughput of over 10 Gbps in more than 40% of our measurement area by applying distributed MIMO.

2) Technology Using CSI Estimation to Transmit Independent Beams between RUs

Figure 5 shows results from testing a technology that transmits independent beams from different RUs by estimating Channel State Information (CSI)*15, which was developed to improve throughput using reflections from buildings. By selecting independent beams from each RU, for example one direct signal and one from a different direction reflected by a building, channel correlation can be reduced, making it possible to increase communication speed. In these experiments, the two beams expected to yield the highest throughput are selected from the four beams with the highest MRSRP by estimating the CSI [8]. The tests assume a street environment where reflections from buildings are common, and were conducted over a roadway between two buildings at the DOCOMO

*15 CSI: Information describing the state of the radio channel.

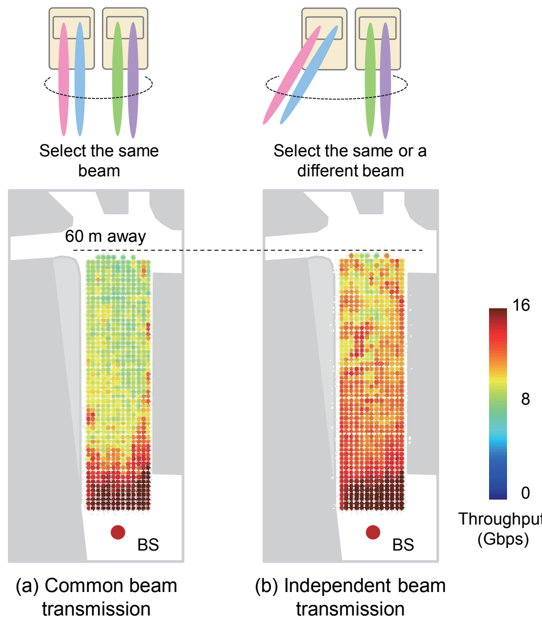

Figure 5 Test results of RU independent beam transmission using CSI estimation

R&D Center. The throughput characteristic when using the same beam for both RUs (i.e. the beam with the highest MRSRP) is shown in Fig. 5 (a), and that when selecting independent beams using CSI estimation is shown in Fig. 5 (b). Comparing the two shows significant improvement in the throughput characteristics for the measured area when selecting independent beams for each RU. Comparing areas in which throughput of 10 Gbps or more was achieved, only about 30% of the area was covered when transmitting the same beam, while over 85% of the area was covered when transmitting independent beams from the two RUs.

This shows that when applying Massive MIMO in high frequency bands, technologies that use multiple transmission points or reflections from buildings are effective in improving communication speeds.

3. Demonstration of 150 km/h High-speed Mobile Data Transmission

The 28 GHz band is promising as a candidate for 5G because ultra-widebands of several hundred MHz can be used, but these bands are difficult to apply to mobile communication because signals are highly directional and propagation losses are large. In the past, NTT DOCOMO collaborated with Samsung Electronics in Korea and successfully tested 28 GHz band MIMO transmission while travelling at 60 km/h [9]. This time, in Japan, to demonstrate the possibility of high-speed wireless data transmission with 5G systems in an even faster mobile environment, we conducted Massive MIMO transmission tests while travelling at 150 km/h, which was the fastest speed ever achieved as of November, 2016. An overview of these tests and the results are given below [10] [11].

3.1 Test Overview

External views of the test equipment are shown in **Figure 6** and the main specifications of the equipment are given in **Table 1**. Both BS and MS have a beam forming function through the use of two sub-arrays. Each sub-array in the BS has 48 antenna elements, implementing Massive MIMO with a total of 96 elements. For each sub-array, the beam with the highest reception power is selected every 10 ms from among the candidates shown in **Figure 7** (8 horizontally × 2 tilt*16 for the BS, 8 horizontally for the MS) to realize beam tracking in a mobile environment. For example, traveling at 150 km/h results in travelling approximately 0.42 m in 10 ms, so at 10 m from the BS, the angular range of motion would be approximately 2.4°. For the BS, which can form a narrower beam than the MS, the beam half-value angle*17 is 10°, so selecting a beam every 10 ms can be expected to track the motion adequately. This equipment supports two-stream MIMO transmission and achieved a maximum transmission rate of 3.77 Gbps using 64QAM*18 with a coding rate*19 of 3/4, and 2.59 Gbps using 64QAM and a coding rate of 1/2.

Transmission tests were conducted at the Fuji Speedway in the town of Oyama, Sunto District, Shizuoka Prefecture. Overhead and horizontal views

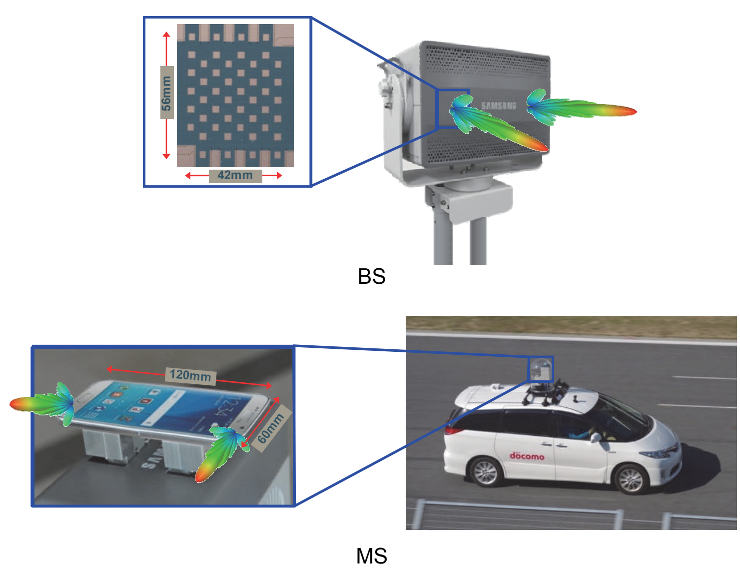

*The SAMSUNG logo is a trademark or registered trademark of Samsung Electronics Co. Ltd.

Figure 6 Equipment external view

---

*16 **Tilt:** Inclination of an antenna's main beam direction in the vertical plane.

*17 **Half-value angle:** The angular range over which the power emitted from an antenna goes from its maximum value to half of that value. Expresses how sharpness of the directivity.

*18 **64QAM:** A digital modulation method that allows transmission of 6 bits of information simultaneously by assigning one value to each of 64 different combinations of amplitude and phase.

*19 **Coding rate:** The proportion of data bits to the number of coded bits after channel coding. For example, if the coding rate is 3/4, for every 3 data bits, 4 coded bits are generated by channel coding.

Table 1　Equipment specifications

Main specifications	BS	MS
Central frequency	27.925 GHz	
Bandwidth	800 MHz	
Duplexing	TDD	
Modulation	64QAM/OFDM	
Channel coding (coding rate)	LDPC coding (1/2, 3/4)	
Antenna elements per sub-array	8 × 6 (=48)	4
Number of sub-arrays	2	2
Spatial multiplicity	2	
Array gain	21 dBi	10 dBi
Transmit power per sub-array	37 dBm	26 dBm

Low-Density Parity Check (LDPC) coding: A type of error correction coding. Linear coding using a sparse parity check matrix with low density non-zero components.

OFDM: Orthogonal Frequency Division Multiplexing

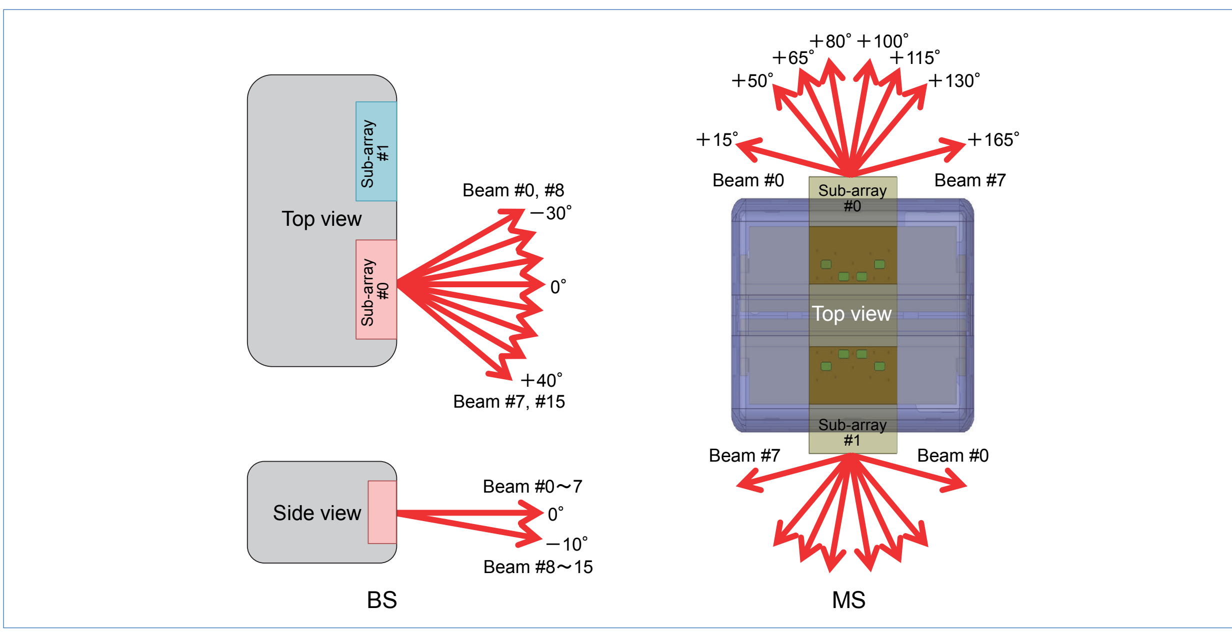

Figure 7　Device beam patterns

of the test environment are shown in **Figure 8**. The home stretch is located between the grand stand and the control center/paddock. The BS was installed in the grand stand, with the tilt angle, θ_{tilt},

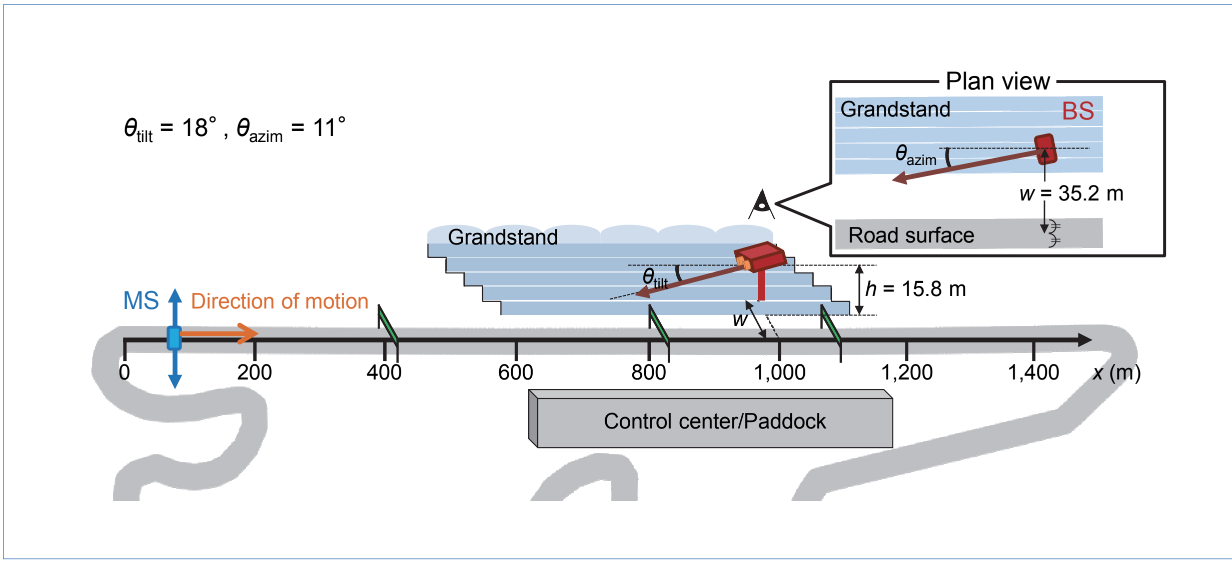

Figure 8 Test environment

of the antenna unit set to 18°, and the azimuth angle, θ_{azim}, set to 11° relative to the direction of the track. The height of the BS antenna was 15.8 m above the track surface. The MS was installed on the roof of the test car with the antennas facing 90° to the direction of movement. The height of the MS antenna was 2.4 m from the track surface. The test vehicle drove along the home stretch from a position approximately 1,000 m from the BS (position x = 0 m).

3.2 Test Results

Measured transmission characteristics are shown in **Figure 9** [10]. Fig. 9 (a) shows throughput when using 64QAM with coding rate fixed at 1/2, and Fig. 9 (b) shows the speed of the MS. The horizontal axis in both cases is the position of the MS along the home stretch. At a coding rate of 3/4, degradation of the transmission characteristic at high speeds was large, so a coding rate of 1/2 was used.

The figure shows that even in the range where speed exceeded 150 km/h, around x = 820 m, high transmission rates of 2.59 Gbps were achieved. On the other hand, in the range of x < 500 m, reception power was low due to attenuation with distance, so the maximum throughput was around 2 Gbps. In this area, there are no particular objects such as buildings to cause reflections, but there should be MIMO transmission, selecting both the direct signal path and the path reflecting from the roadway. In the region of 500 m < x < 900 m, reception power increases as the MS approaches the BS, so even in the range where the MS speed exceeded 150 km/h, the maximum throughput, according to specifications, of 2.59 Gbps was obtained. In this region, the direct path and a path reflecting from buildings (paddock, etc.) could be used effectively, so even with LOS, MIMO transmission was possible. Note that near x = 700 m,

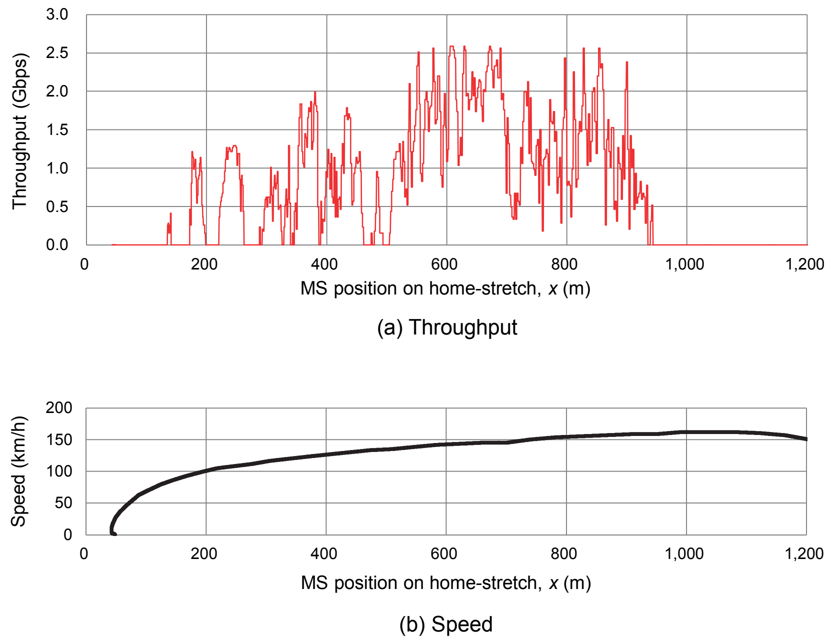

Figure 9 High-speed mobility test results

the effects of gates positioned on the home stretch blocked the direct signal path, causing sudden degradation of throughput. However, the adaptive modulation and coding*20 and rank adaptive control*21 functions were able to mitigate the sudden drop in throughput [11]. Also, for $x > 900$ m, the MS was outside of the range covered by the beam of the BS, located at $x = 1{,}000$ m, so the throughput dropped greatly.

4. Demonstration of Further Improvements in Spectral Efficiency

So far, we have introduced results of tests done in high frequency bands over 6 GHz, but there are also 5G candidate bands below 6 GHz, relatively close to bands currently in use. In these bands it is difficult to secure widebands approaching 1 GHz, so to realize the ultra-high-speed and high capacity communications required for 5G, spectral efficiency must be greatly increased. NTT DOCOMO has been testing Massive MIMO transmission technology to improve spectral efficiency using the 4.5 GHz band in the Minato Mirai 21 District of Yokohama City, in collaboration with Huawei Technologies [12] [13]. An overview of these tests and their results is given below.

4.1 Test Overview

The specifications of equipment used in this test are shown in **Table 2**. The 4.5 GHz band was used and system bandwidth was 200 MHz. External

*20 **Adaptive modulation and coding:** A method of modifying the modulation and coding schemes according to radio propagation path conditions. Modulation and coding schemes are modified to increase reliability when the propagation environment is poor, and to increase throughput when it is good.

*21 **Rank adaptive control:** A method that changes the number of spatially multiplexed streams adaptively according to the state of the radio propagation path. If the propagation environment has a large number of eigenspaces (rank), which are needed for spatial multiplexing, the number of spatially multiplexed streams is increased to obtain higher throughput.

Table 2 Equipment specifications

Item	Value
Frequency band	4.55 - 4.75 GHz
Subcarrier interval	15 kHz
TTI length (slot length)	0.5 ms
Number of OFDM symbols per TTI	7
CP length	Long CP: 5.2 μs (160 samples) Short CP: 4.17 μs (128 samples)
Modulation encoding format	LTE
System bandwidth	200 MHz
Bandwidth per CC	20 MHz
Number of subcarriers per CC	1,320 (110 RB)
Number of subcarriers in entire system	1,320 × 10
Slot structure ratio (Normal)	DL : S : UL = 5 : 1 : 1
Slot structure ratio (Special)	DL : S : UL = 4 : 2 : 1
Number of antenna elements	BS: 192, MS: 8
Antenna element intervals	BS: 3.72 cm × 5.21 cm, MS: 12.5 cm
Antenna tilt angle	16.4°
Antenna installation height	BS: 108 m, MS: 3.2 m
Maximum transmission power	BS: 46 dBm, MS: 23dBm
Maximum number of transmission streams	3 per MS, 24 per BS

CC: Component Carrier

CP: Cyclic Prefix

TTI: Transmission Time Interval

views of the BS and MS, and the location of BS installation in the test environment are shown in **Figure 10**. The BS antenna equipment used in these tests consisted of 64 antenna units (8 horizontally, 4 vertically, 2 polarizations) and each antenna unit consisted of three antenna elements. Thus, the BS had a Massive MIMO antenna structure with 192 antenna elements. Antenna height was approximately 108 m, and tilt was 16.4° (10.4° mechanical, 6° electrical tilt). The MS antenna structure was an eight-element linear array antenna*22, with antenna elements at approximately 12.5 cm intervals. BS and MS had maximum transmission power of 46 dBm and 23 dBm respectively. The maximum number of transmit streams per MS for downlink MIMO transmission was three, and the maximum number of

*22 Linear array antenna: An antenna with antenna elements arranged at fixed intervals in a straight line.

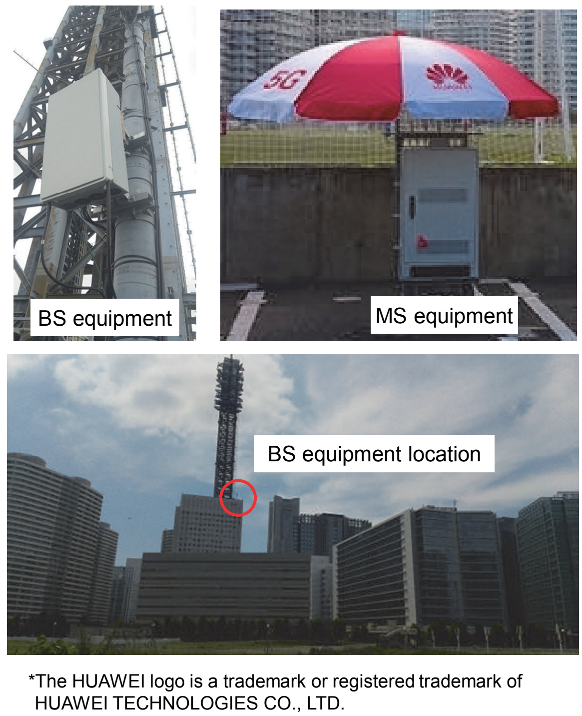

Figure 10 External views of BS and MS

simultaneous transmit streams per BS to multiple MS using MU-MIMO was 24.

To generate orthogonal beams without interference between MU-MIMO streams or MSs, Eigen Zero Forcing (EZF)*23 was used as a precoding*24 method, which uses Singular Value Decomposition (SVD)*25 of the propagation channels. Here, channel reciprocity*26 between uplink and downlink with Time Division Duplex (TDD)*27 can be used to estimate propagation channels, which is to say that the uplink signal can be used to estimate the downlink propagation channel. To maintain reciprocity between uplink and downlink channels, we introduced RF calibration*28 of up and down links on the base station.

The test environment is shown in **Figure 11**. The maximum distance from BS to MS was 590 m, and the test area was approximately 100,000 m^2, the largest 5G transmission test environment in Japan. Within the test area, an MS simulating a high-end terminal, using the maximum bandwidth of 200 MHz, was placed at one location (MS11 in the figure), and pairs of MSs, using the upper and lower 100 MHz of the 200 MHz total bandwidth respectively, were placed at each of the other 11 locations. Thus, a total of 23 MS devices were placed in the test

---

*23 EZF: A technique used with precoding and beam forming in the transmitter, in which the generalized inverse of the channel matrix is used to generate weighting coefficients such that interference between users goes to zero.

*24 Precoding: With MIMO, a process of multiplying the signal by weightings suited to the radio propagation path before it is transmitted in order to improve reception quality.

*25 SVD: In linear algebra, a matrix decomposition method for matrices with real or complex components.

*26 Reciprocity: The state in a bidirectional transceiver in which each received signal is affected in the same way. For example, using TDD and a carrier with the same Radio Frequency (RF) on both the uplink and a downlink, assuming there is no interference, channel fluctuation in the received signals of both the base station and the mobile station will be the same, resulting in transmission path reciprocity.

area. The test involved LOS measurements, and MS were arranged to ensure at least 50 m vertically and horizontally between MSs using the same frequency.

4.2 Test Results

These tests evaluated the MU-MIMO system throughput characteristics (total throughput for all MSs). The output screen showing the measured result from the test equipment is shown in **Figure 12**. The

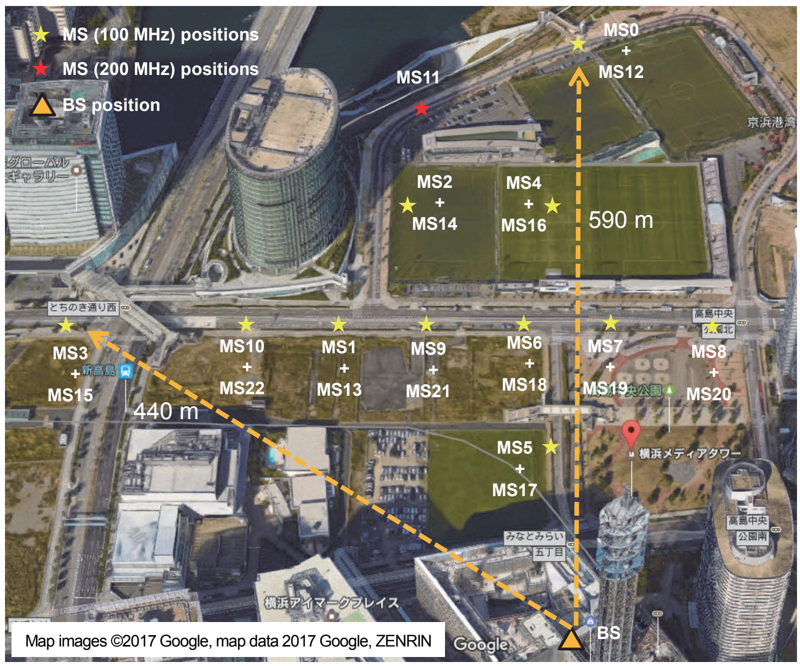

Figure 11　Test environment

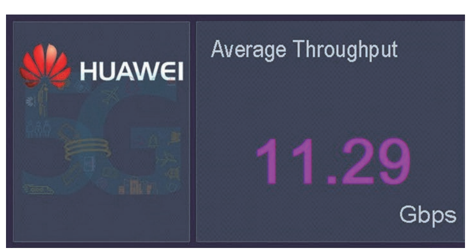

*The HUAWEI logo is a trademark or registered trademark of HUAWEI TECHNOLOGIES CO., LTD.

Figure 12　Test equipment measurement results

*27　TDD: A bidirectional transmit/receive mode, which achieves bidirectional communication by allocating different time slots to uplink and downlink transmissions that use the same frequency.

*28　Calibration: Pre-correction of imbalance in characteristics among antennas when arranging multiple antenna elements, etc. to emit signals in a suitable manner.

result shows that the average throughput per second peaked at 11.29 Gbps, verifying that in large-scale MU-MIMO transmission, TDD up/down link channel reciprocity can be used. This is equivalent to 79.82 bps/Hz/cell when converting to spectral efficiency, which is approximately five-times the theoretical spectral efficiency of LTE-Advanced 4 × 4 MIMO in frequency bands below 6 GHz (which is 15 bps/Hz/cell).

The throughput characteristics per MS are shown in **Figure 13**. They show that simultaneous communication with 23 MSs was supported, providing 500 Mbps-class throughput to all MSs without significant variation, and providing throughput of approximately 800 Mbps to the high-end MS (MS11) using 200 MHz bandwidth.

5. Conclusion

This article has introduced the most significant new test results on 5G transmission, which NTT DOCOMO has been conducting in collaboration with major global equipment vendors. We will continue to promote study and testing to establish radio technologies for 5G and its extension (5G+*29) in the future. Starting in May 2017, we plan to develop a new service and content utilizing 5G, called "5G Trial Site," in broad collaboration with industry partners, and to build an environment that will enable ordinary users to experience 5G [14] [15].

REFERENCES

[1] 5GPPP: "Second Global 5G Event on 9-10 November 2016, Rome (Italy)."
https://5g-ppp.eu/event/second-global-5g-event-on-9-10-november-2016-in-rome-italy/

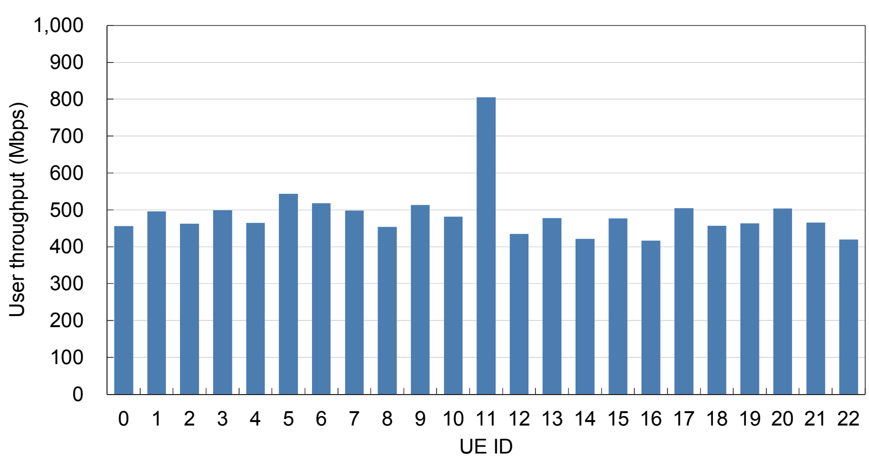

Figure 13 User throughput characteristics and testing results

*29 5G+: An abbreviation expressing development beyond 5G.

[2] Y. Kishiyama et al.: "NTT DOCOMO 5G Activities—Toward 2020 Launch of 5G Services—," NTT DOCOMO Technical Journal, Vol.17, No.4, pp.4–15, Apr. 2016.

[3] S. Suyama et al.: "5G Multi-antenna Technology," NTT DOCOMO Technical Journal, Vol.17, No.4, pp.29–39, Apr. 2016.

[4] A. Harada et al.: "5G Trials with Major Global Vendors," NTT DOCOMO Technical Journal, Vol.17, No.4, pp.60–69, Apr. 2016.

[5] NTT DOCOMO Press Release: "DOCOMO and Ericsson Succeed in World's first trial to achieve a cumulative 20Gbps with two simultaneously connected mobile devices in 5G Outdoor Trial," Feb. 2016.
https://www.nttdocomo.co.jp/english/info/media_center/pr/2016/0222_03.html

[6] K. Tateishi, D. Kurita, A. Harada, Y. Kishiyama, S. Itoh, H. Murai, S. Parkvall, J. Furuskog and P. Nauclér: "5G Experimental Trial Achieving Over 20 Gbps Using Advanced Multi-antenna Solutions," IEEE VTC2016-Fall, Sep. 2016.

[7] D. Kurita, K. Tateishi, A. Harada, Y. Kishiyama, S. Itoh, H. Murai, A. Simonsson and P. Ökvist: "Indoor and Outdoor Experiments on 5G Radio Access Using Distributed MIMO and Beamforming in 15 GHz Frequency Band," IEEE Globecom 2016 WS, Dec. 2016.

[8] K. Tateishi, D. Kurita, A. Harada and Y. Kishiyama: "Performance Analysis on Beam Tracking Using CSI Feedback for 5G Radio Access," IEICE Technical Report, Vol.116, No.383, RCS2016-231, pp.129–134, Dec. 2016.

[9] T. Obara, Y. Inoue, Y. Aoki, S. Suyama, J. Lee and Y. Okumura: "Experiment of 28 GHz Band 5G Super Wideband Transmission Using Beamforming and Beam Tracking in High Mobility Environment," IEEE PIMRC, Sep. 2016.

[10] K. Satoh, J. Mashino, S. Suyama, Y. Inoue and Y. Okumura: "Outdoor Experiment of 28 GHz-band Super Wide Bandwidth Massive MIMO Transmission for 5G – High Mobility Experiment in Fuji Speedway (1) –," IEICE General Conference, B-5-76, Mar. 2017.

[11] J. Mashino, K. Satoh, S. Suyama, Y. Inoue, Y. Okumura: "Outdoor Experiment of 28 GHz-band Super Wide Bandwidth Massive MIMO Transmission for 5G – High Mobility Experiment in Fuji Speedway (2) –," IEICE General Conference, B-5-77, Mar. 2017.

[12] Y. Saito, A. Benjebbour, Y. Kishiyama, X. Wang, X. Hou, H. Jiang, L. Lu, B. Li, W. Liang, L. Gu, Y. Cui and T. Kashima: "Investigation on the Performance of TDD Massive MIMO in the 4.5GHz Band," IEICE Technical Report, Vol.116, No.396, RCS2016-240, pp.25–30, Jan. 2017.

[13] Y. Saito, A. Benjebbour, Y. Kishiyama, X. Wang, X. Hou, H. Jiang, L. Lu, B. Li, W. Liang, L. Gu, Y. Cui and T. Kashima: "Experimental trial of large scale downlink TDD multi-user Massive MIMO," IEICE Technical Report, Vol.116, No.479, RCS2016-323, pp.187–192, Mar. 2017.

[14] NTT DOCOMO Press Release: "DOCOMO to Launch 5G Trial Environments that Enable Customers to Experience New Services and Content—Will Collaborate with Ericsson and Intel on Initial 5G Trial Sites—," Nov. 2016.
https://www.nttdocomo.co.jp/english/info/media_center/pr/2016/1109_00.html

[15] NTT DOCOMO: "5G Trial Site."
https://www.nttdocomo.co.jp/corporate/technology/rd/docomo5g/trial_site/index.html

Technology Reports

Head-mounted Display VR Field-of-view

Expanding Viewing Angle in Head-mounted Displays Considering Field-of-view Characteristics

Research Laboratories Wataru Yamada Hiroyuki Manabe

The market for head-mounted displays is growing dramatically. A head-mounted display provides a sense of immersion and presence, but to deepen these features, the viewing angle must be widened. This, however, has generally required multiple displays and complicated optics in which manufacturing cost and weight have been issues. Focusing on the differences between central vision and peripheral vision, NTT DOCOMO has developed a technique for expanding the viewing angle of a head-mounted display at low cost with a lightweight configuration by using an arrangement of lenses with different levels of magnification.

1. Introduction

A Head-Mounted Display (HMD) is a type of display device worn on the head to present images or video to the user. Many consumer-oriented HMDs have recently come on the market thanks to price reductions in high-definition displays and high-performance CPUs and GPUs.

HMDs displays like PlayStation® VR*1 and Google Cardboard™*2 shown in **Figure 1** are called "immersion-type" or "non-transparent-type" in which a non-transparent display is placed in front of the user's eyeballs to present images.

At present, such commercially available immersion-type HMDs can be further divided into two main types depending on the implementation format.

(1) The first type (hereinafter referred to as "integrated HMD") comes equipped with displays and CPUs that are specially designed for HMDs. The PlayStation VR mentioned above is an integrated HMD.

(2) The second type (hereinafter referred to as "add-on HMD") provides only a case and

*1 PlayStation® VR: A VR system marketed by Sony Interactive Entertainment Inc. PlayStation and its logo are registered trademarks of the same.

*2 Google Cardboard™: A head-mounted display provided by Google, Inc. and a trademark or registered trademark of the same.

(a) PlayStation VR

(b) Google Cardboard

*SONY and the SONY logo are registered trademarks of Sony Corporation

Figure 1　Examples of commercially available HMDs

lenses as in the Google Cardboard viewer. It can be used as an HMD by then inserting a smartphone into the viewer. The greatest advantage of an add-on HMD is that it can be achieved at very low cost since it enables users to use their own smartphones that they are already familiar with. On the other hand, while an integrated HMD enables the use of a specialized high-resolution display for each eye, an add-on HMD can mount only one display since it uses an ordinary smartphone. Such a display has not been designed particularly for an HMD. As a result, the performance of an add-on HMD is inferior to that of an integrated HMD that can mount displays having specialized dimensions and resolution.

The performance of an HMD can be evaluated by a variety of criteria, but a particularly important one is viewing angle. This is an index of the user's range of vision when wearing an HMD. In a Virtual Reality (VR) environment, a wide viewing angle can give rise to discomfort or nausea, i.e., VR sickness, but it can also deepen a sense of immersion and presence [1]. "Immersion" is the extent to which the user has a sense of being in the VR environment, while "presence" is the extent to which objects or persons appear to be in the VR environment. Both immersion and presence can have a big effect on the quality of the user experience in a VR environment, so achieving a wide viewing angle to improve these sensations has been the subject of much research for some time.

Many of those studies, however, assumed the need for complicated optics (a generic term for devices and equipment using refraction, reflection, etc.) and multiple displays, so achieving a practical design was difficult because of jumps in cost and weight among other reasons.

Against the above background, NTT DOCOMO has proposed a technique for expanding the viewing angle of an HMD at low cost with a lightweight configuration by focusing on human field-of-view characteristics [2]. In addition to convex lenses placed in front of both eyes, this technique surrounds each of those lenses with a Fresnel lens*3 having a higher level of magnification. As a result, the user is presented with a blurred image in the peripheral visual field through the Fresnel lenses thereby expanding the viewing angle. In this article, we describe this technology and proposed technique.

2. Human Field-of-view Characteristics and Related Technology

2.1 Central and Peripheral Vision

Although there are a variety of opinions, the human field of view is generally said to be approximately 180 degrees in the horizontal direction and 90 degrees in the vertical direction. On the other hand, a human being does not recognize all objects within that field of view equally. The field of view of a person closely observing some object can be divided into central vision that includes that object and its neighborhood and peripheral vision that covers the area outside of the above. It is known that central vision and peripheral vision have different features regarding shape and color perception, response to temporal changes, etc. [3]. One of these features is resolution. Compared with central vision, the resolution of peripheral vision in humans is low resulting in only fuzzy recognition.

The research of HMDs focusing on this feature has been proposed.

2.2 Related Technology

Xiao et al. [4] proposed an HMD equipped with arrays of full-color Light Emitting Diodes (LEDs) and a diffuser sheet*4 placed around the convex lenses in front of the user's eyes.

In that research, the colors of the LEDs surrounding the convex lenses are synchronized with the image within the HMD, and the synchronized light irradiates the user's peripheral visual field making it appear as an image with low resolution. For the user, this has the effect of expanding the viewing angle. This technique makes use of the fact that such a low-resolution image does not detract from the naturalness of the entire image given that the user is capable of only fuzzy recognition in peripheral vision. In addition, this technique requires no complicated optics or great increase in weight, but it does require many electronic components including a number of full-color LEDs and a microcontroller for image/LED synchronization processing as well as a battery to drive the above. Applying this technique to an add-on HMD is therefore difficult in terms of manufacturing cost.

2.3 Proposed Technique

Taking the above issues into account, NTT DOCOMO proposes a technique for expanding the viewing angle of an HMD at low cost with a lightweight configuration by using two sets of lenses with different levels of magnification. This technique can be applied to either an integrated HMD or add-on HMD. As in the technique of Xiao et al., the proposed technique makes use of the characteristic

*3 **Fresnel lens:** A lens that refracts and diffuses or concentrates light through the use of concentrically etched grooves. It features a thin, lightweight configuration compared with ordinary lenses.

*4 **Diffuser sheet:** A sheet that diffuses irradiating light and weakens optical directionality.

that the user is capable of only fuzzy recognition in peripheral vision.

A prototype device implementing the proposed technique is shown in **Figure 2**. As shown, this prototype is equipped with two types of lenses having different levels of magnification. The first type consists of convex lenses placed in front of both eyes. These convex lenses (focal length*5: 44 mm; diameter: 25 mm) are provided to present a clear image in the user's central visual field. The other type consists of Fresnel lenses (focal length: 25 mm; dimensions: W70 × H68 × D2 mm) with high magnification that surround the convex lenses. These high-magnification Fresnel lenses are provided to fill the peripheral visual field with a blurred image that the user can only vaguely recognize. The following can also be offered as a reason for using Fresnel lenses. Since the size of the display is limited, the magnification factor must be increased and the lens itself made larger to present an image on a broader scale. With convex lenses, however, increasing the magnification factor also increases lens thickness thereby increasing lens weight. Fresnel lenses, in contrast, can remain thin and light even when increasing the magnification factor, so this is another reason for their adoption. In addition, the center of each lens lies 39 mm from the surface of the corresponding display.

This mechanism can be explained using glasses for near sightedness as an analogy. While the scenery seen through the glasses appears clear and distinct, the area outside the glasses appears blurred to the user. However, if this blurred area outside the glasses cannot be seen at all, the user will sense a narrow field of view. In other words, the proposed technique achieves a wide viewing angle by starting with a convex lens portion corresponding to the inner side of such glasses and then adding high-magnification Fresnel lenses for generating an image in the area corresponding to

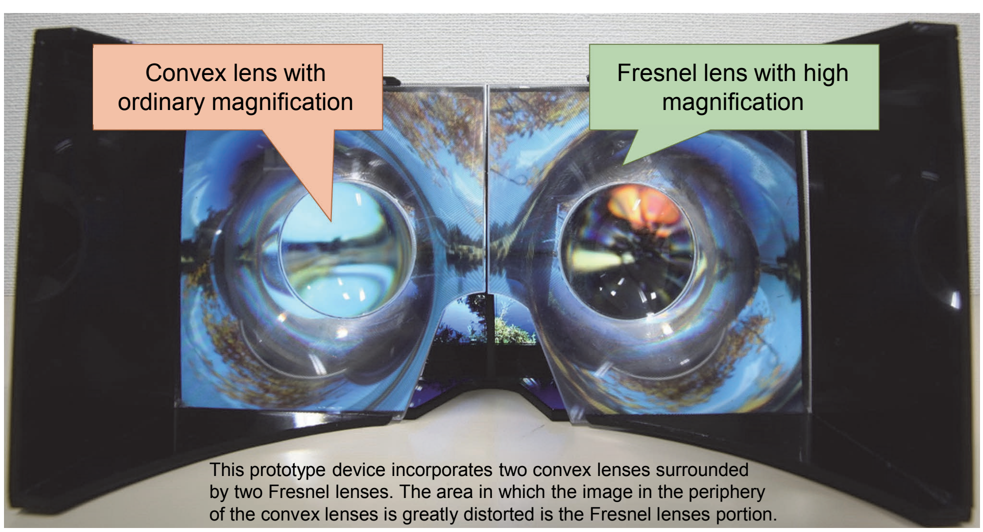

Figure 2 Prototype device

*5 Focal length: For a convex lens, parallel light incident along the optical axis of the lens will focus at a certain point called the focal point. The distance from this point to the lens center is the focal length.

the outer side of the glasses. We note here that the photo in the figure was taken at a distance from the prototype, so while the image in the Fresnel lens portion is greatly distorted, it will not appear as such when actually wearing the device.

A close-up photo of the prototype device equipped with both convex lenses and Fresnel lenses is shown in **Figure 3** (a) and that with the Fresnel lens portion replaced by an opaque black panel is shown in Fig. 3 (b). In either case, the photo was taken with the focal point lying on the display seen through a convex lens. Although the image seen through the convex lens in either photo appears clear, a blurred image can be seen through the Fresnel lens in Fig. 3 (a), but in Fig. 3 (b), the area surrounding the convex lens is black. In this way, a user wearing a prototype device based on the proposed technique will be presented with a blurred image in peripheral vision resulting in a wider viewing angle as shown in Fig. 3 (a).

A blurred image presented in peripheral vision has several characteristics. For example, the Fresnel lenses through which the user sees an image in peripheral vision have a shorter focal length than the convex lenses, so a portion of the image appears to be duplicated and discontinuous across the convex and Fresnel lenses (Fig. 3 (a)). Moreover, the image seen through the Fresnel lenses is expanded at high magnification with the result that the boundaries of individual pixels on the display would normally become noticeable. In actuality, though, the blurred appearance of the image seen through the Fresnel lenses tends to conceal those boundaries making them barely visible for the most part.

As described above, the proposed technique can widen the viewing angle in an ordinary add-on HMD by adding high-magnification Fresnel lenses

(a) Prototype device equipped with both convex and Fresnel lenses

(b) Prototype device replacing the Fresnel lens with an opaque black panel

Figure 3　Close-up photo of convex lens in prototype device

and filling peripheral vision with a blurred image. The main feature of this technique is that only two types of lenses with different levels of magnification are needed with no need for complicated optics or electronic parts. It is therefore a superior approach from the viewpoint of cost and weight. There is also no need for specialized image-reproduction software, which means that existing content can be appropriated as-is. This is another strong point of the proposed technique from the viewpoint of practical use.

3. Conclusion

In this article, we described a technique for expanding viewing angle of an HMD at low cost with a lightweight configuration by using lenses with two different levels of magnification. In future research, we plan to research and develop a more detailed design for the optical system and to study the commercialization of this technique toward new VR services while promoting advancements in this technology.

REFERENCES

[1] J. J.-W. Lin, H. B. L. Duh, D. E. Parker, H. Abi-Rached and T. A. Furness: "Effects of field of view on presence enjoyment memory and simulator sickness in a virtual environment," In Proc. of IEEE Virtual Reality 2002, pp.164–171, Mar. 2002.

[2] W. Yamada and H. Manabe: "Expanding the Fields-of-View of Head-Mounted Displays with Peripheral Blurred Images," In Adjunct Proc. of 29th Annual ACM Symposium on User Interface Software and Technology, pp.141–142, Oct. 2016.

[3] Y. Ishiguro and J. Rekimoto: "Peripheral Vision Annotation: Noninterference Information Presentation Method by Using Gaze Information," Transactions of Information Processing Society of Japan, Vol.53, No.4, pp.1328–1337, Apr. 2012 (in Japanese).

[4] R. Xiao and H. Benko: "Augmenting the Field-of-View of Head-Mounted Displays with Sparse Peripheral Displays," In Proc. of the 2016 CHI Conference on Human Factors in Computing Systems, pp.1221–1232, May 2016.

Flexible Display | Rollable Type Device Concept | Responsive Web Design

Topics

Future Smartphone Concept with Flexible Display Offering New UX

Communication Device Development Department **Makoto Takimoto**

Recently, foldable and flexible displays have been developed and announced by several display manufacturers [1], and devices equipped with such displays will be seen in the smartphone market in the coming years. Some smartphones on the market today already have displays that curve around the edges [2], and many patents for flexible smartphone display technologies have been filed and published.

In light of this trend, NTT DOCOMO has been considering the future possibilities of these flexible display technologies, and has conceived a new rollable type flexible smartphone display. In addition, we have also developed a User Interface (UI) technology that changes size by expanding and retracting the rollable display.

This article describes the basic ideas and the motivation behind the rollable type smartphone concept, and also describes development (prototyping) of the UI technology, which aims to offer new User eXperiences (UXs)*1.

In this development, we utilized the "foldable display®*2" [3] provided by Semiconductor Energy Laboratory Co., Ltd. as the flexible display panel (**Table 1**).

1) Objective of This Development

This development focused on achieving a future-oriented device concept and smartphone UI to offer an attractive UX that will enable users to imagine the promise and wonder of future mobile communication services.

2) Study of Device Concept Design

The flexible display can be folded, twisted and rolled. In studying the flexible display device concept, we thought that the device should:

- Maximize advantages and features of the flexible display,
- Offer a view into the future with the sense of promise and surprise,

Table 1 Foldable display specifications

Display size	8.7 inch
Resolution	1,920 × 1,080 pix
Foldable radius of curvature	2 mm
Repeated folding	100,000 folds or more*

*With radius of curvature of 2 mm.

*1 UX: A general term for the experiences gained through the use or consumption of certain products or services.

*2 foldable display®: A registered trademark of Semiconductor Energy Laboratory Co., Ltd.

- Be practical for ease of development and handling.

As a result of the above studies and taking potential usability improvements into consideration, we came up with two promising concepts - the tri-fold type and the rollable type, as described below.

(1) As shown in **Figure 1**, the tri-fold type can be folded to a third of its size to become a normal smartphone or expanded to its full size to become a tablet device.

(2) As shown in **Figure 2**, the rollable type smartphone can be retracted to the size of a normal smartphone or freely extended from the smartphone size to a tablet size.

On comparing the above two types, we chose the rollable type for the prototyping, as it more closely met our UI/UX development aims.

3) UI Technology Development for the Rollable Type Smartphone

As mentioned, the rollable type concept typically offers two device sizes, smartphone or tablet, and also enables users to enjoy any display size they like between the two. Hence, to create attractive and convenient UXs for this future smartphone concept, we came up with a new UI technology to display content and its layout dynamically to fit the varied display size (**Figure 3**).

- Installation of a potentiometer*3

To achieve the above idea, we attached a potentiometer to the scrolling rod of the flexible display panel to sense how much the display panel is rolled up, which enables calculation of the size of the display.

- Applying Responsive Web Design

With the flexible optimized UI design, it is crucial that display content fit the varying display size. Hence, we decided to leverage Responsive Web Design technology with HyperText Markup Language 5 (HTML5)*4 and Cascading Style Sheets 3 (CSS3)*5 since they are already

*3 **Potentiometer:** An element that senses the amount of rotation and movement.

*4 **HTML5:** The 5th and current version of the HTML standard markup language used for structuring and presenting content on the World Wide Web.

*5 **CSS3:** The level 3 version of the Cascading Style Sheets language used for describing the presentation of a document written in a markup language.

Figure 1　Tri-fold type

Figure 2　Rollable type

widely used. In Web browsers on PCs, Responsive Web Design changes the content size and layout to fit the width of the Web browser window size. Thus, we adapted this technology for the aforementioned variable size of this rollable type smartphone flexible display.

- Flow for displaying content

The following describes the operation of components in the device, and the flow for displaying content on the rollable device.

(a) Calculation of the display size of the rollable device

The amount of display expansion/retraction is sensed by the potentiometer in the scrolling rod of the display panel, and the row data is fed to the UI software (**Figure 4** (1)).

If the sensed data exceeds a certain threshold, the UI software calculates the display size from the sensed data value and the diameter of the wound up display panel

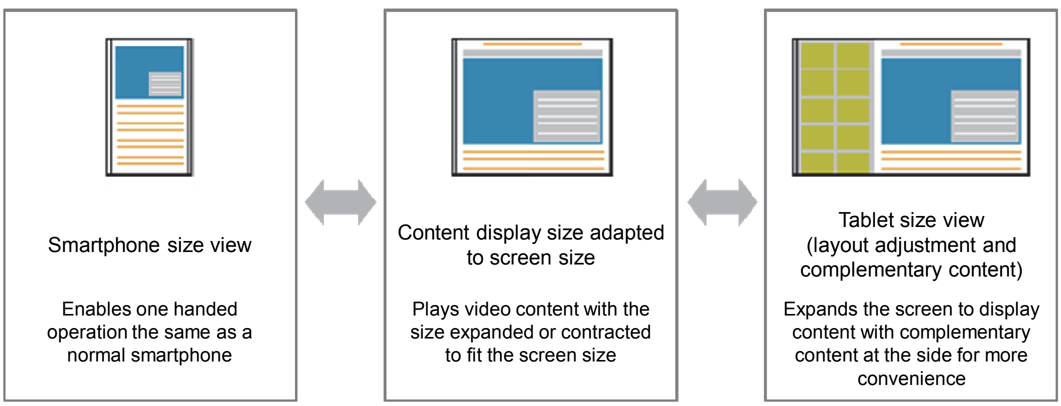

Figure 3 Flexible UI optimized for the display size

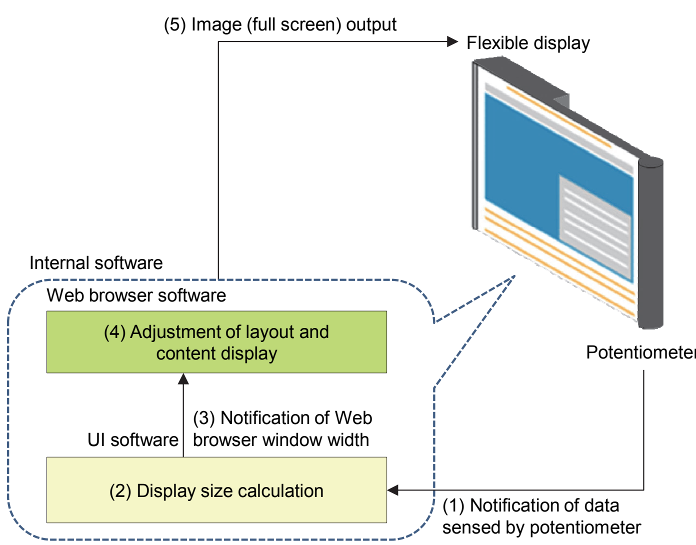

Figure 4 UI adjustment mechanisms

(Fig. 4 (2)), and then the calculated display size is fed to the Web browser as the width of Web browser window size (Fig. 4 (3)).

(b) Adjustment of content layout and display

Because most of content and Web browsers support the Responsive Web Design function, the layout and the display of the content can be adjusted to fit the width of the Web browser window ((Fig. 4 (4)).

(c) Display on the flexible display

After the above adjustment, the Web browser window is output with the window width matched to the size of the flat part of the flexible display, which is fed from the UI software as mentioned above (Fig. 4 (5)). By repeating (a) to (c) above, the device can display content by changing the content size to match the screen size of the rollable display as it is extended or retracted.

With the above, we successfully developed a UI that optimally and dynamically displays content to fit the variable display size (**Photo 1**).

Through the above development, we achieved a prototype[*6] of a rollable flexible display device concept that can be held in the hand, and by developing UI technology optimized for this concept device, we achieved a new, attractive and convenient UX that gives the user the sense of the promise and wonder of the mobile communications services of the future.

To commercialize smartphones with this flexible display, robustness of the device (drop resistance, etc.) and the flexible display (scratch hardness, cover film solution, etc.) must be studied in consideration of usage in various scenes.

In addition to the above studies, we will be engaging in further studies to offer even more attractive

*6 **Prototype:** An early sample, model, or release of a product to test and evaluate a concept.

Video playback with the normal smartphone size

Content size adjusted to extended display size

Video playback with the tablet size

Layout changes in further extended display size. Includes complementary content (links) on the left of the main content

Photo 1　Developed prototype

and convenient UXs to provide promising and surprising services to users.

REFERENCES

[1] N. Tanaka: "Flexible LCD challenging organic EL in the main battlefield," Nikkei Electronics, 2016 / 07 issue, pp.44-49, Jul. 2016 (In Japanese).

[2] NTT DOCOMO: "Galaxy S7 edge SC-02H," (In Japanese). https://www.nttdocomo.co.jp/product/smart_phone/sc02h/topics_01.html?icid=CRP_PRD_sc02h_topics_up

[3] Semiconductor Energy Laboratory Co., Ltd: "OS display - R&D." https://www.sel.co.jp/en/technology/os_display.html

Film-type Wideband Multiband Antenna for M2M Device

Research Laboratories　Yasunori Suzuki　Makoto Sumi

Corporate Sales and Marketing Department II　Hiroaki Oda

With the advancement of Internet and mobile telephone technologies, the use of Machine to Machine (M2M)*1 services is on the rise both in Japan and around the world. Both moving objects such as vehicles and fixed objects such as production machinery are being monitoring with M2M devices. Also, although mobile telephone frequency bands used in many countries are mostly the same, the frequency bands used for M2M services are different in some countries. Hence, with vehicles such as trucks, monitoring with M2M devices might be done using different frequency bands across various countries.

Due to these circumstances, M2M wireless modules must support various wireless systems, and must be equipped with wideband, multiband antennas to handle multiple frequency bands. Furthermore, there are demands for antennas with better installability due to the limited positions and space in which antennas can be mounted in vehicles and on industrial equipment.

In addition, some M2M devices might be used in areas of insufficient radio signal level depending on the operating conditions of the vehicles or industrial equipment. For this reason, high gain antennas are required to enable stable communications in weak radio signal areas.

To meet these demands, NTT DOCOMO has developed a film-type wideband, multiband antenna for M2M devices that supports mobile telephone frequency bands and Wi-Fi®*2. This article outlines the configuration of the film-type wideband multiband antenna and examples of its potential uses.

1) Antenna Configuration

(1) Array antenna

The film antenna introduced in this article adopts an array antenna*3 structure to achieve high gain on multiple bands. **Figure 1** shows the elemental antennas. Fig. 1 (a) shows a low band (800 - 900 MHz)/high band (1,700 - 2,600 MHz, Wi-Fi) combination wideband-type achieved in one element, while Fig. 1 (b) shows a high band-type achieved with one high band element, with the low band element (800 - 900 MHz) omitted from the wideband-type. Both of these elements are designed based on the dipole antenna*4.

Base stations usually have plenty of space to install antennas, and so the low band and high band arrays are usually in different positions.

*1 M2M: Machine-to-Machine Communications between machines. Systems that enable machines to communicate with each other without any human mediation.

*2 Wi-Fi®: A registered trademark of the Wi-Fi Alliance.

*3 Array antenna: An antenna consisting of multiple elements.

*4 Dipole antenna: The simplest of all antenna configurations. The ends of the cable (feeding point) are connected to two straight conductors (antenna elements).

However, due to the space constraints common with M2M antennas, space is saved by positioning the low band and high band arrays in the same place (**Figure 2**). Generally, the distance between elements of array antennas is 0.5 to 0.9 wavelengths, although this depends on the number of elements. Also, directivity*5 gain is maximum with an element spacing of 0.8 to 0.9 wavelengths, however this falls rapidly if exceeded due to the effects of grating lobes*6. Considering this characteristic, configurations with different numbers of elements are used for the different frequencies, three-element arrays for high bands, and two-element arrays for low bands. This is because with a three-element low band array, the normalized wavelength spacing of the elements becomes small due to the long low-band wavelength, therefore the radiative pattern substantially deteriorates and the gain falls. Also, optimizing each elemental spacing in advance suppresses the effects of grating lobes and maximizes gain in all bands.

(2) Using PET (PolyEthylene Terephthalate) sheet

Designed to be attached to vehicle glass, this

*5 Directivity: An antenna radiation characteristic indicating the directional characteristics of radiation strength (or reception sensitivity) from the antenna.

*6 Grating lobe: The radiative pattern of a linear array of evenly spaced antenna elements is determined by the distance between the elements, the number of elements and the beam scanning amount. Certain combinations radiate and can be measured in visible regions of actual space, although some combinations create large lobes (beams) in visible regions separate from the main lobe radiating in the desired direction in invisible regions, which reduces gain in the desired direction. These unwanted lobes are called grating lobes.

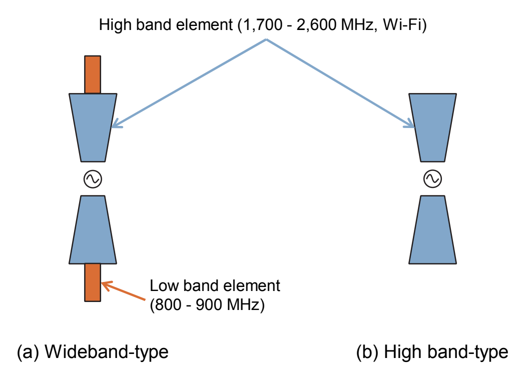

Figure 1 Elemental antennas (images)

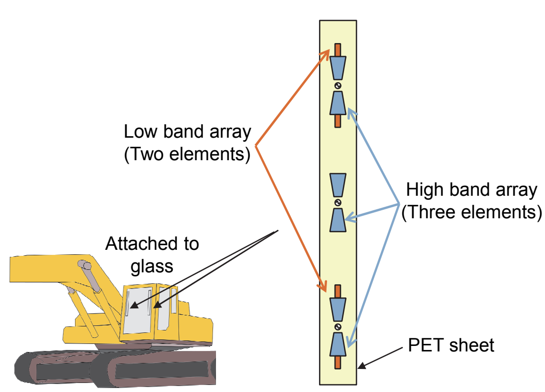

Figure 2 Film-type wideband multiband antenna

antenna uses a 0.1 mm PET sheet instead of the usual printed substrate. Also, the antenna elements are optimized in consideration of the dialectic constant of the glass.

(3) Power combiner

We developed a power combiner for the feed circuit of the antenna to provide two-way power combining functions for the lower-band array antenna and three-way power combining functions for the higher-band array antenna to suit the developed array antenna structure. This power combiner has three ports, with one port having a notch filter to suppress the higher-band frequency signal. This enables the power combiner to output the lower-band and higher-band frequency signals to two and three ports respectively, and hence effectively combine both signals. The output port of the power combiner is fed into the input port of M2M module. The power combiner for receiving signals can also operate as a power divider for transmitted signals.

2) Usage Cases

Making use of thinness and transparency of the film antenna, the following examples of practical application can be considered.

- Glass surfaces of automobiles etc.

  As infotainment*7 is gradually becoming more popular, presumably it will become more common to enjoy video content in passenger and rear seating in vehicles while on the move, which means attachment of this antenna to glass surfaces will preserve visibility in the limited space available in vehicles.

- Monitoring equipment

  As monitoring equipment installed on roadways is designed in consideration of the landscape, film could enable remote monitoring without compromising the landscape by devising ways to install it in certain locations.

- Others

  Depending on the way it's attached, film could also enable anti-theft measures. As well as that, the extensive use of glass in construction in recent years also holds prospects for advantageous applications of this technology.

This article has outlined a film-type wideband, multiband antenna developed to support mobile telephone frequency bands and Wi-Fi. The structure of this array antenna achieves never-before-seen high gain, and uses PET sheeting for excellent installability. As well as being attachable to glass, the technology aims to enable stable communications with M2M devices used all over the world. In the future, this technology has potential to play a role in the expansion of global use of M2M devices.

REFERENCE

[1] The Institute of Electronics, Information and Communication Engineers: "Antenna Engineering Handbook (2nd Edition)," Ohmsha, Ltd., pp.399-409, 2008 (In Japanese).

*7 Infotainment: Services that provide combined information and entertainment. For example, this could refer to combined services that enable on-board music and video appreciation as well as access to map and traffic congestion information.

A Translation Add-in for Microsoft Office for Easy-to-use Machine Translation in Business Scenes

Service Innovation Department Takashi Shimizu Yuki Chidiwa Takaya Ono

To achieve communications that transcend the language barrier, NTT DOCOMO provides "Hanashite Hon'yaku," "Mail Hon'yaku," "Utsushite Hon'yaku," "Jspeak" and "Tegaki Hon'yaku" consumer-oriented translation services. NTT DOCOMO also provides "Hanashite Hon'yaku for Biz" as a translation service aiding businesses in the support they provide to overseas visitors to Japan. The services have been designed for use in all aspects of everyday life and travel situations.

However, as globalization of business continues, opportunities and demands to exchange business documents and e-mail created in languages other than one's own native language are increasing.

To translate such documents, mostly (1) the services of a translator are employed, or (2) a Web-based machine translation service is used.

(1) is time consuming and involves monetary costs.

(2) does not take much time and is low-cost, but at least involves uploading files from a browser or copying and pasting the text to be translated into a text box in a browser. Thus, operating both a word processor application and a browser can be an involved task.

In addition, documents in business scenes are characterized as follows.

(a) With application forms or slides etc., not only the text but the layout may also have meaning.

(b) Creating e-mail may entail frequent additional corrections to text and so forth.

(c) The wide range of business types and occupations may require specific styles and terms used for translation.

Hence, machine translation in business must (a) not affect layout, (b) have functions to aid text creation and (c) have excellent translation accuracy*1 matched to the type of business or occupation.

In light of these circumstances, to achieve easy-to-use machine translation of business documents and e-mail in foreign languages, NTT DOCOMO and Mirai Translate, Inc. jointly studied an add-in*2 for Microsoft® Office®*3, a well-known software package widely used for business document and e-mail creation. This add-in was developed and is sold by Mirai Translate [1].

Combining the add-in and machine translation software, we have included operations required for

*1 Translation accuracy: In this article, "translation accuracy" refers to the combination of degree of detail conveyed in the translation, the fluency of the translation, and the degree of adequacy of the translation to the target field (style, suitability of specialist terminology etc.).

*2 Add-in: A program to add a function to an existing software application.

*3 Microsoft® Office®: A trademark or registered trademark of Microsoft Corp. in the United States and other countries.

translation in Microsoft Office applications to shorten the time it takes to acquire a translation.

In this article, we describe the add-in functions we have developed, and methods of improving the accuracy of translation.

1) Add-in Functions

Figure 1 shows how the add-in is included in Microsoft® PowerPoint®*4.

As shown in fig. 1, when the add-in is installed, a tab called "Mirai Translation" containing buttons necessary for translation is added to the ribbon. Here, the user can specify the source and target languages for translation (Original and Translation) and a translation model, discussed later.

After specifying the languages and translation model, the user can specify translation targets from three patterns - entire document, selected page only, or selected statements only. With translation of entire document or selected page only, the results of translation are output to a file separate from the original.

Figure 2 describes the flow of translation

*4 Microsoft® PowerPoint®: A trademark or registered trademark of Microsoft Corp. in the United States and other countries.

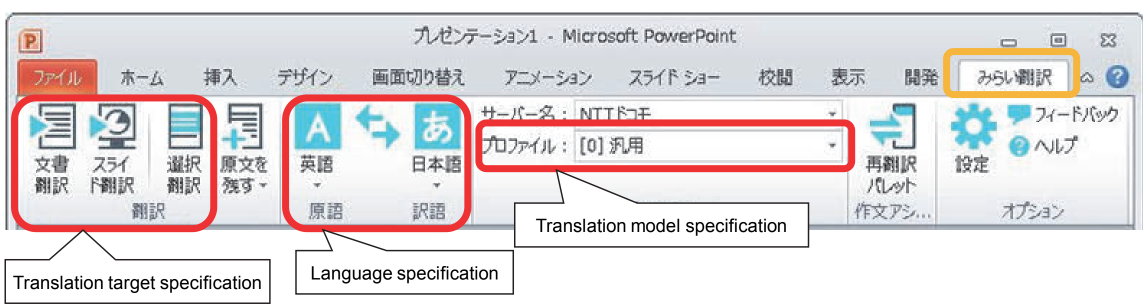

Figure 1 Add-in deployment image

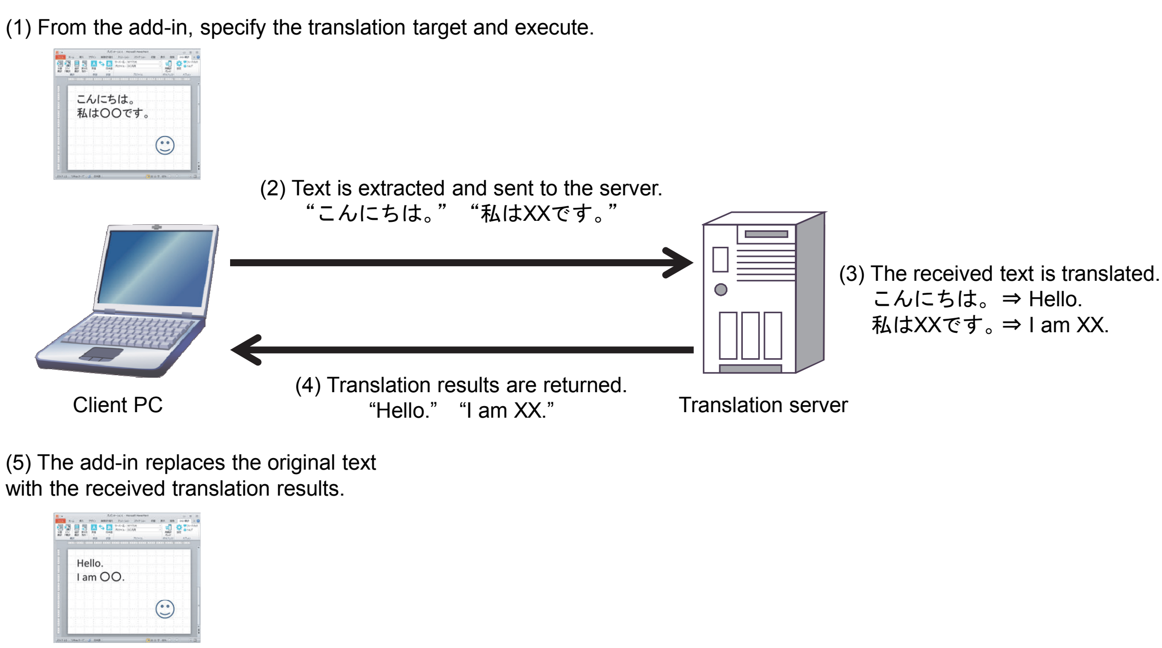

Figure 2 Translation process flow

processing with this add-in. When the target for translation is specified, processing begins (Fig. 2 (1)). The add-in extracts the text in the document and sends it to a translation server (Fig. 2 (2)). The translation server translates it with the specified languages and the selected translation model (Fig. 2 (3)), and returns the results of translation to the add-in (Fig. 2 (4)). When the add-in receives the translation results, it replaces the original text with the translation results (Fig. 2 (5)). This processing enables translation while maintaining formats such as complex document layouts and bold text etc. Also, it is possible to keep the original text with selected statements only as the target for translation.

As well as providing machine translation for the text entered, the add-in also has assistance functions for creating e-mail (in Microsoft® Outlook®*5) that list example statements preregistered in the add-in that are similar to the text entered. If the list contains a useful expression, the user can write by selecting the example statement, without using the machine translation (**Figure 3**).

2) Improving Translation Accuracy

Because this add-in is designed for business documents and e-mail, we made improvements to specialize in these areas.

(1) One is leveraging the aforementioned translation model. A translation model gives probabilities to combinations of words and their translation, which is adjusted according to the type of statements. For example, it is possible to improve the accuracy of translation compared to generic translation by selecting a translation model that handles unique expressions used in specialized documents such as patents. In addition, it is also possible to further tune translation models to suit an individual company using bilingual text owned by the company and the usage log of the add-in.

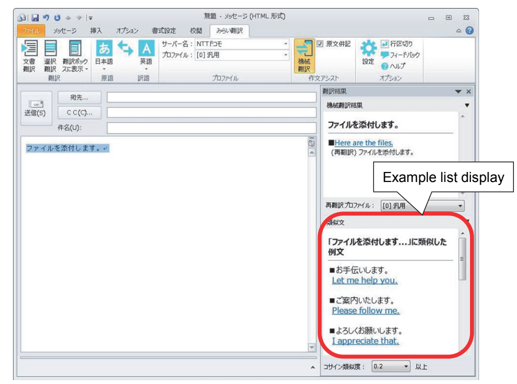

Figure 3 Assistance for creating statements in Outlook

(2) Other improvements are the use of dictionaries in which product and service names, and industry-specific terms etc. are registered, and the registration and use of fixed phrases if such wording exists. Since such registered terms and phrases include many business and industry-specific terms and phrases, there is potential for unknown words*6 or mistranslations occurring, which we have attempted to rectify with registration in dictionaries and lists of fixed phrases.

This article has described the functions of a Microsoft Office translation add-in designed for business documents and e-mail, and improvements to translation accuracy. Moving forward, we will take initiatives to further improve convenience and translation accuracy.

REFERENCE

[1] Mirai Translate: "Product introduction | Mirai Translate | Innovative machine translation," (in Japanese). https://miraitranslate.com/products/office

---

*5 Microsoft® Outlook®: A trademark or registered trademark of Microsoft Corp. in the United States and other countries.

*6 Unknown word: A word not in a translation model or dictionary. These are often proper nouns.

NTT DOCOMO
Technical Journal Vol.19 No.1

Editorship and Publication
NTT DOCOMO Technical Journal is a quarterly journal edited by NTT DOCOMO, INC. and published by The Telecommunications Association.

Editorial Correspondence
NTT DOCOMO Technical Journal Editorial Office
R&D Strategy Department
NTT DOCOMO, INC.
Sanno Park Tower
2-11-1, Nagata-cho, Chiyoda-ku, Tokyo 100-6150, Japan
e-mail: dtj@nttdocomo.com